Chemistry – A European Journal

Supporting Information

Tuning NIR Absorption and Emission of Diphenyl-dihydrophenazine-Based Merocyanines with Ultra Narrow Band Gap

Kateřina Teichmanová[a,b], Stanislav Luňák Jr.[f], Karel Pauk[b], Lukáš Střižík[e], Zdeňka Růžičková[e], Tomáš Mikysek[d], Klára Melánová[c], Aleš Imramovský[b]*, Kazuhiko Nagura[a]*

[a]Research Center for Materials Nanoarchitectonics (MANA), National Institute for Materials Science (NIMS), 1-1 Namiki, 304-0044 Tsukuba, Ibaraki, Japan

[b]Institute of Organic Chemistry and Technology, Faculty of Chemical Technology, University of Pardubice, Studentská 95, 53210 Pardubice, Czech Republic

[c]Center of Materials and Nanotechnologies, Faculty of Chemical Technology, University of Pardubice, Studentská 95, 532 10 Pardubice, Czech Republic

[d]Department of Analytical Chemistry, Faculty of Chemical Technology, University of Pardubice, Studentská 95, 53210 Pardubice, Czech Republic

[e]Department of General and Inorganic Chemistry, Faculty of Chemical Technology, University of Pardubice, Studentská 95, 53210 Pardubice, Czech Republic

[f]Materials Research Centre, Faculty of Chemistry, University of Technology, Purkyňova 464, 612 00 Brno, Czech Republic

Contents

S1 General experimental methods

Synthesis and characterization

All starting materials and reagents were purchased from commercial suppliers and used without further purification. Reactions were monitored by using thin-layer chromatography (TLC) plates coated with 0.2 mm silica gel (60 F254, Merck). TLC plates were visualized by using UV irradiation (254 nm and 365 nm). Column chromatography was performed using silica gel 60 N (spherical, neutral, Kanto Chemical Co., Inc.). Target compounds were further purified by recycling preparative high-performance liquid chromatography HPLC LC-9225NEXT (Japan Analytical Industry, JAI) equipped with JAIGEL-2HH and 1HH columns by using chloroform as an eluent at room temperature. All melting points were determined by using a Melting Point B-540 apparatus (Büchi, Switzerland) and are given in their uncorrected form. Spectroscopic grade solvents (cyclohexane, toluene, 1,4-dioxane, THF, dichloromethane, chloroform, acetonitrile, methanol and DMSO) were used for all spectroscopic studies. NMR spectra were measured in DMSO-d_6, CD_2Cl_2, C_6D_6, $CDCl_3$ solutions at ambient temperature on a JEOL ECZ-400S spectrometer at frequencies 399.78 MHz (^{1}H) and 100.26 MHz (^{13}C{^{1}H}) or on a Bruker AscendTM 500 spectrometer at frequencies 500.13 MHz (^{1}H) and 125.76 MHz (^{13}C{^{1}H}). The chemical shifts (δ) reported in the Experimental section and Supporting Information are given in ppm and are related to the following residual solvent peaks: 2.50 (DMSO-d_6), 5.32 (CD_2Cl_2), 7.16 (C_6D_6) and 7.27 ($CDCl_3$). The coupling constants (J) are reported in Hz. Mass spectrometry with high resolution was determined by the “dried droplet” method using a MALDI mass spectrometer LTQ Orbitrap XL (Thermo Fisher Scientific) equipped with a nitrogen UV laser (337 nm, 60 Hz) or Bruker micrOTOF II spectrometer with the atmospheric-pressure chemical ionization (APCI) method. Mass spectra were measured in positive ion mode and in regular mass extent with a resolution of 100000 at a mass-to-charge ratio (m/z) of 400, with 2,5-dihydrobenzoic acid (DBH) used as a matrix. MS spectra in reflectron mode were obtained on a Shimadzu AXIMA Confidence MALDI-TOF-MS using dithranol as a matrix.

S2 Synthesis and characterization

5,10-dihydrophenazine

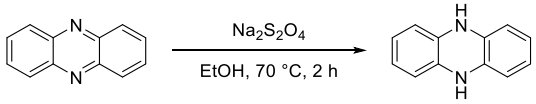

5,10-dihydrophenazine was synthesized according to a slightly modified published procedure [S1] as follows:

In a 1L round-bottomed flask, phenazine (15.0 g, 82.3 mmol, 1.00 eq.) was dissolved in absolute ethanol (300 mL) and heated to 70 °C. A solution of $Na_2S_2O_4$ (150 g, 0.862 mol, 10.0 eq.) in 350 mL of distilled water was added over a period of 10 min, leading to formation of a pale green precipitate. The mixture was stirred at 70 °C for two hours. After cooling to room temperature, the crude precipitate was filtrated off and washed thoroughly with distilled water. After drying under reduced pressure, it was obtained 14.7 g of **5,10-dihydrophenazine** as pale green powder (97%). The next step was proceeded immediately without any further purification.

R_f: 0.35 (*n*-hexane/EtOAc = 3/1, v/v). **^{1}H NMR** (500 MHz, DMSO-d_6): δ 7.29 (s, 2H), 6.27 (m, 4H), 6.00 (m, 4H). **^{13}C NMR** (126 MHz, DMSO-d_6): δ 133.7, 120.2, 111.3. Obtained data are in good agreement with literature [S1].

5,10-diphenyl-dihydrophenazine

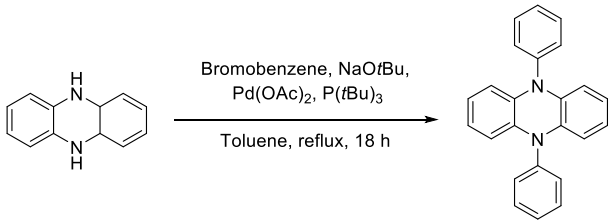

DPPZ

5,10-diphenyl-dihydrophenazine was synthesized according to the published procedure [S2].

To an oven-dried 250 mL three-necked flask containing 5,10-dihydrophenazine (5.00 g, 27.4 mmol, 1.00 eq.), NaO*t*Bu (8.00 g, 82.3 mmol, 3.00 eq.), $Pd(OAc)_2$ (0.240 g, 1.09 mmol, 0.04 eq.), bromobenzene (5.74 ml, 54.9 mmol, 2.00 eq.) and P(*t*Bu)$_3$ (0.18 mL, 0.82 mmol, 0.03 eq.) were dispersed in toluene (150 mL) and resulting mixture was refluxed under nitrogen atmosphere for 18 h. After cooling to room temperature, reaction was quenched by adding 80 mL of water. The organic phases were separated, and the aqueous layer was extracted with ethyl acetate (3 × 100 mL). Collected organic phases were dried over Na_2SO_4 and evaporated under reduced pressure. The crude product was purified by column chromatography (mobile phase ethyl acetate/*n*-hexane 1/7). It was obtained 4.80 g of **5,10-diphenyl-dihydrophenazine** as yellowish powder (52%).

R_f: 0.55 (*n*-hexane/EtOAc = 7/1, v/v), **m.p.** 285.0–285.5 °C. **^{1}H NMR** (400 MHz, C_6D_6): δ 7.17–7.13 (m, 8H, overlapped with solvent signal), 7.02–7.00 (m, 2H), 6.28–6.24 (m, 4H), 5.83–5.78 (m, 4H). **^{13}C NMR** (101 MHz, C_6D_6): δ 140.8, 137.2, 131.6, 131.5, 127.1, 121.4, 113.1. **HRMS**: $[M]^+$ Calcd. for $C_{24}H_{18}N_2$: 334.14654; found 334.14647. Obtained data are in good agreement with literature [S2].

2-(2,3-dihydro-1H-inden-1-ylidene)malononitrile (ID)

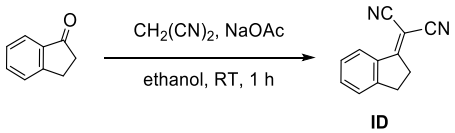

ID

2-(2,3-dihydro-1*H*-inden-1-ylidene)malononitrile was synthesized according to a published procedure [S3].

In a 250 mL round-bottomed flask, a mixture of 1-indanone (5.00 g, 37.8 mmol, 1.00 eq.), malononitrile (3.15 mL, 50.0 mmol, 1.32 eq.) and sodium acetate (3.10 g, 37.8 mmol, 1.00 eq.) was stirred in absolute ethanol (30 mL) at room temperature for 1 hour. Resulting mixture was diluted with water (30 mL) and then acidified with 1M HCl (10 mL) followed by precipitation of white solid. After filtration, washing with cold ethanol and recrystallization from ethanol, it was obtained 1.24 g of compound **ID** as white crystals (18%).

R_f: 0.29 (*n*-hexane/EtOAc = 3/1, v/v), **m.p**. 153.0–153.5 °C. **^{1}H NMR** (500 MHz, CD_2Cl_2): δ 8.38 (d, J = 8.1 Hz, 1H), 7.62 (t, J = 7.7 Hz, 1H), 7.51 (d, J = 7.8 Hz, 1H), 7.44 (t, J = 7.7 Hz,

1H), 3.28–3.25 (m, 2H), 3.23 – 3.16 (m, 2H). **^{13}C NMR** (126 MHz, CD_2Cl_2): δ 180.0, 155.0, 136.2, 135.5, 128.5, 126.8, 126.4, 114.1, 113.6, 74.7, 35.2, 30.2. **HRMS:** [M^+] Calcd. for $C_{12}H_8N_2$ 203.05797; found 203.05816. Obtained data are in good agreement with literature [S3].

2-(3-oxo-2,3-dihydro-1*H*-inden-1-ylidene)malononitrile (IDO)

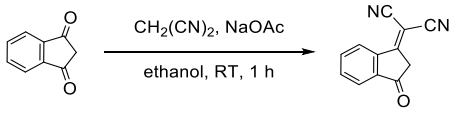

IDO

2-(3-oxo-2,3-dihydro-1*H*-inden-1-ylidene)malononitrile was synthesized according to a published procedure [S4].

In a 100 mL round-bottomed flask, a mixture of 1,3-indandione (2.00 g, 13.7 mmol, 1.00 eq.), malononitrile (1.15 mL, 18.26 mmol, 1.33 eq.) and sodium acetate (1.34 g, 16.4 mmol, 1.17 eq.) was stirred in absolute ethanol (30 mL) at room temperature for 1 hour. Resulting mixture was diluted with water (30 mL) and then acidified with concentrated HCl (pH = 1–2) followed by precipitation of brown solid. After filtration, washing with water and recrystallization from acetic acid, it was obtained 1.92 g of compound **IDO** as brown powder (73%).

R_f: 0.33 (*n*-hexane/MeOH = 1/1, v/v), **m.p.** 222.0–223.0 °C. **^{1}H NMR** (400 MHz, C_6D_6): δ 8.15–8.13 (m, 1H), 7.40–7.38 (m, 1H), 6.85–6.77 (m, 2H), 2.54 (s, 2H). **^{13}C NMR** (101 MHz, C_6D_6): δ 194.1, 165.8, 142.3, 140.5, 134.9, 134.5, 125.6, 123.8, 112.7, 112.2, 79.2, 42.5. **HRMS**: $[M+H+(DHB)]^+$ Calcd. for $C_{19}H_{13}N_2O_5$ 349.08135; found 349.08249. Obtained data are in good agreement with literature [S4].

(Indan-1,3-diylidene)dimalononitrile (IDD)

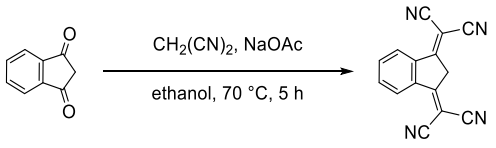

IDD

(Indan-1,3-diylidene)dimalononitrile was synthesized according to a published procedure [S4].

In a 200 mL round-bottomed flask, a mixture of 1,3-indandione (3.60 g, 24.6 mmol, 1.00 eq.), malononitrile (6.90 mL, 109.5 mmol, 4.45 eq.) and sodium acetate (1.90 g, 125 mmol, 1.00 eq.) in absolute ethanol (60 mL) was stirred at 70 °C for 5 hours. After cooling to room temperature, resulting mixture was diluted with water (40 mL) and then acidified with concentrated HCl (pH = 1–2) followed by precipitation of dark brown solid. After filtration, washing with water and recrystallization from acetic acid, it was obtained 3.70 g of compound **IDD** as dark brown powder (62%).

R_f: 0.44 (*n*-hexane/MeOH = 1/1, v/v), **m.p.** 255.2–256.0 °C. **^{1}H NMR** (400 MHz, $CDCl_3$): δ 8.68–8.63 (m, 2H), 7.94–7.88 (m, 2H), 4.30 (s, 2H). **^{13}C NMR** (101 MHz, $CDCl_3$): δ 165.3, 140.6, 136.3, 127.0, 111.8, 111.6, 79.3, 41.9. **HRMS**: $[M+H+(DHB)]^+$ Calcd. for $C_{22}H_{13}N_4O_4$ 379.09259; found 379.09393. Obtained data are in good agreement with literature [S4].

S3 ^{1}H and ^{13}C NMR spectra of synthesized compounds

S3.1 ^{1}H NMR of 5,10-dihydrophenazine

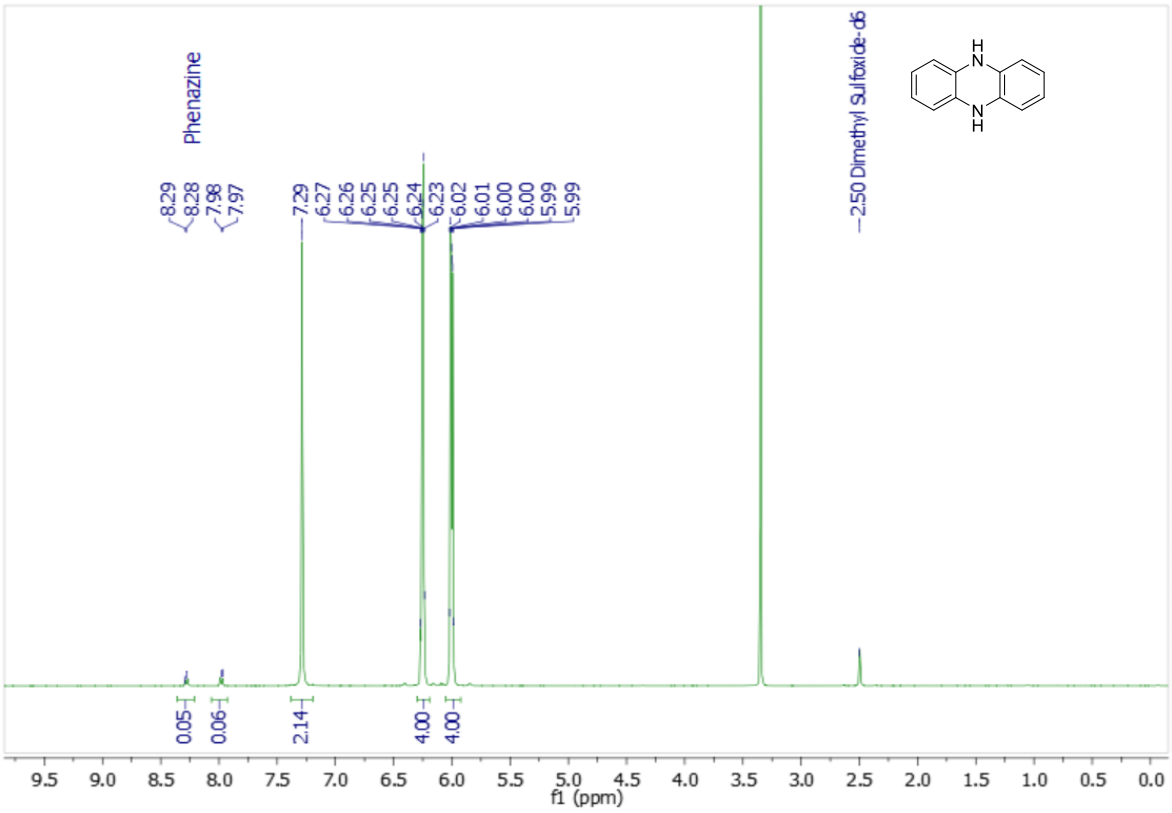

^{13}C NMR of 5,10-dihydrophenazine

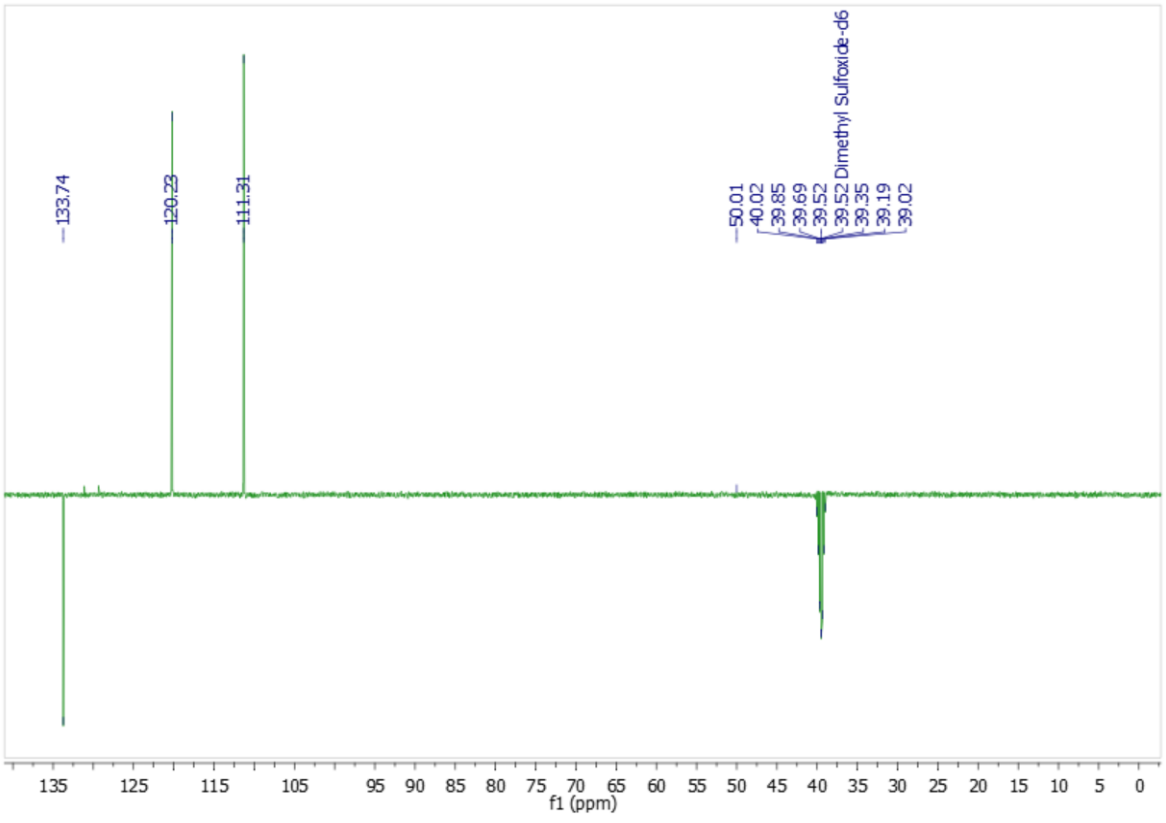

S3.2 ^{1}H NMR of diphenyl-5,10-dihydrophenazine

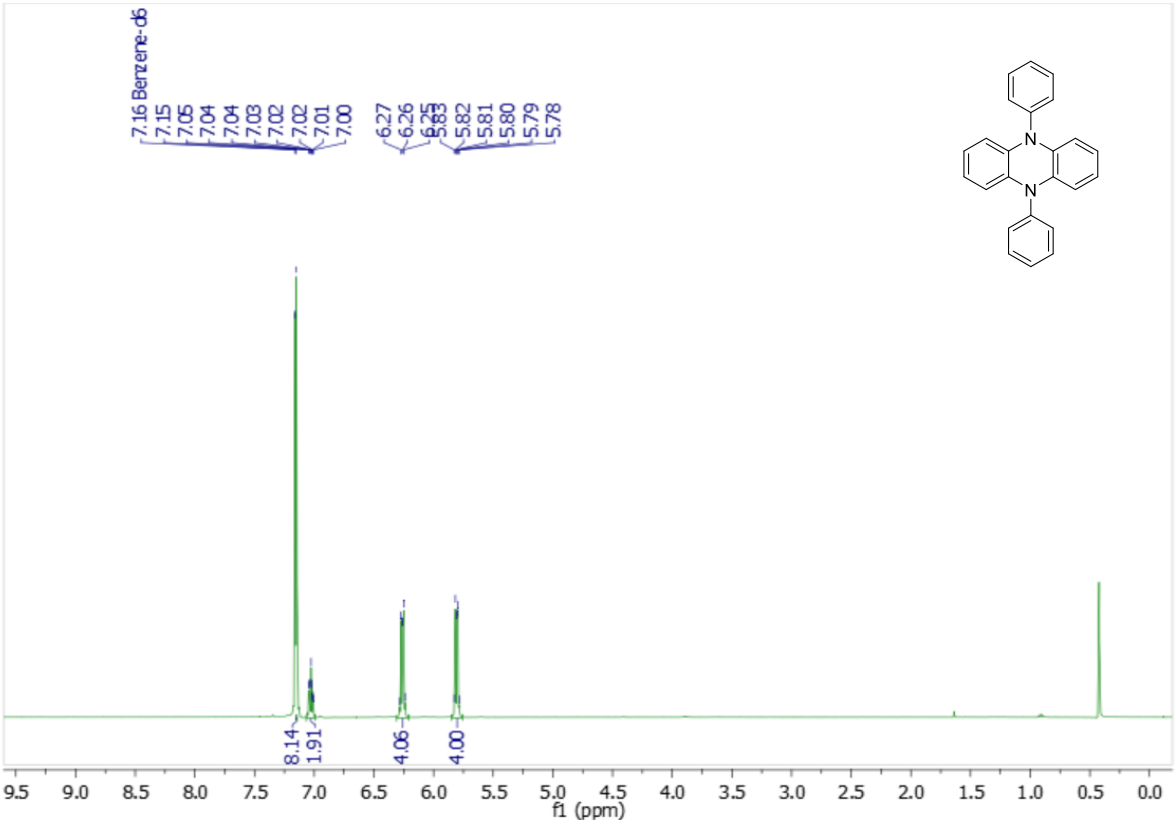

^{13}C NMR of diphenyl-5,10-dihydrophenazine

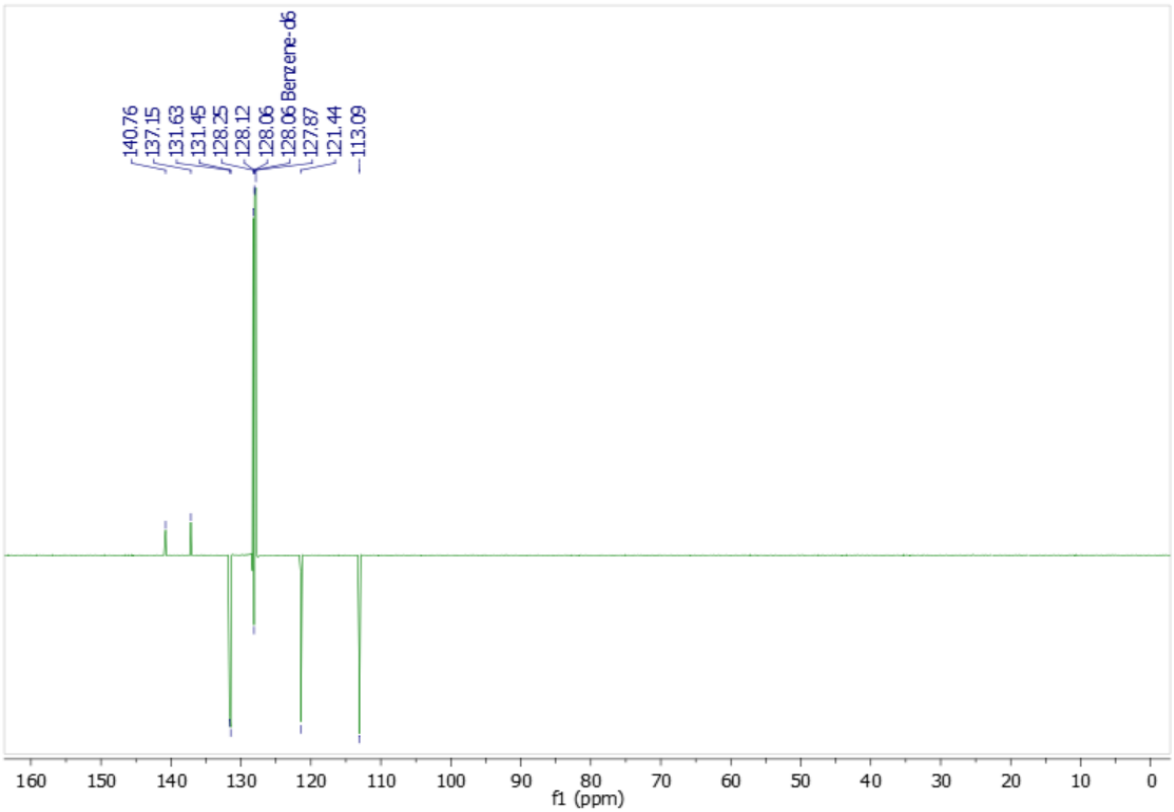

S3.3 ^{1}H NMR of 2-(2,3-dihydro-1*H*-inden-1-ylidene)malononitrile (ID)

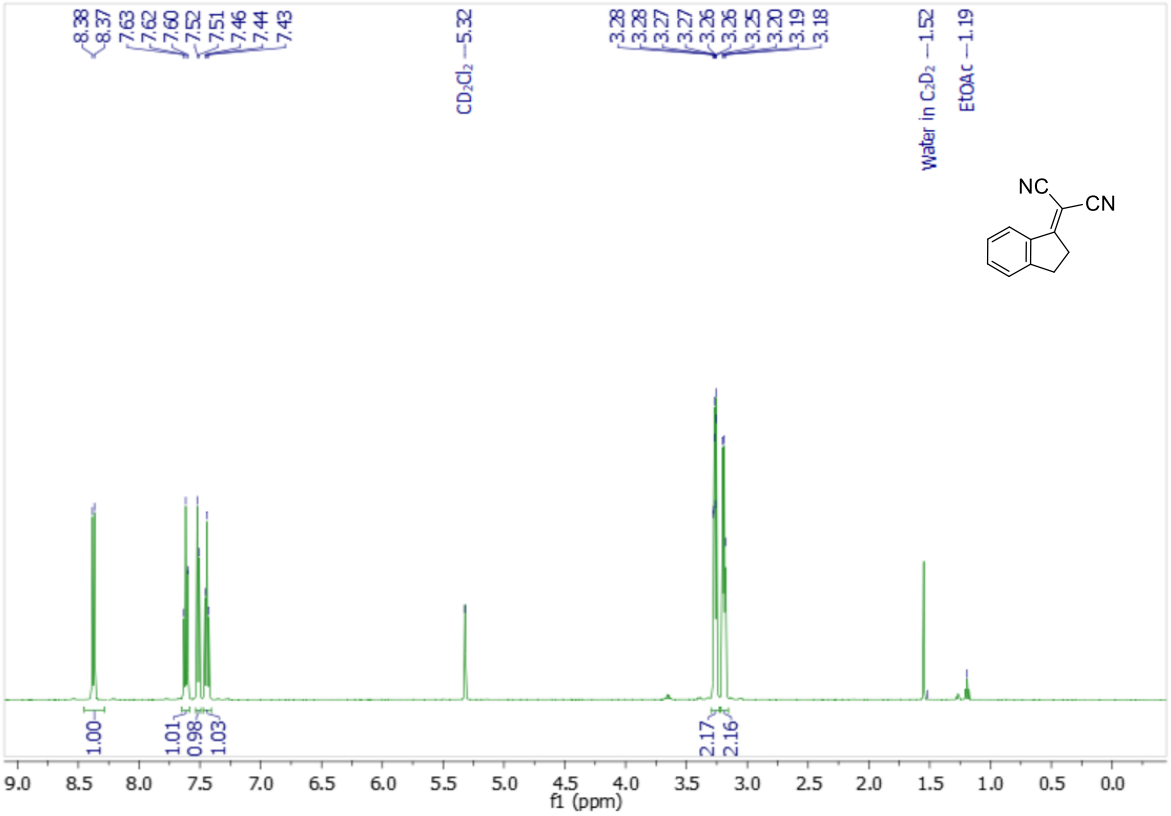

^{13}C NMR of 2-(2,3-dihydro-1*H*-inden-1-ylidene)malononitrile (ID)

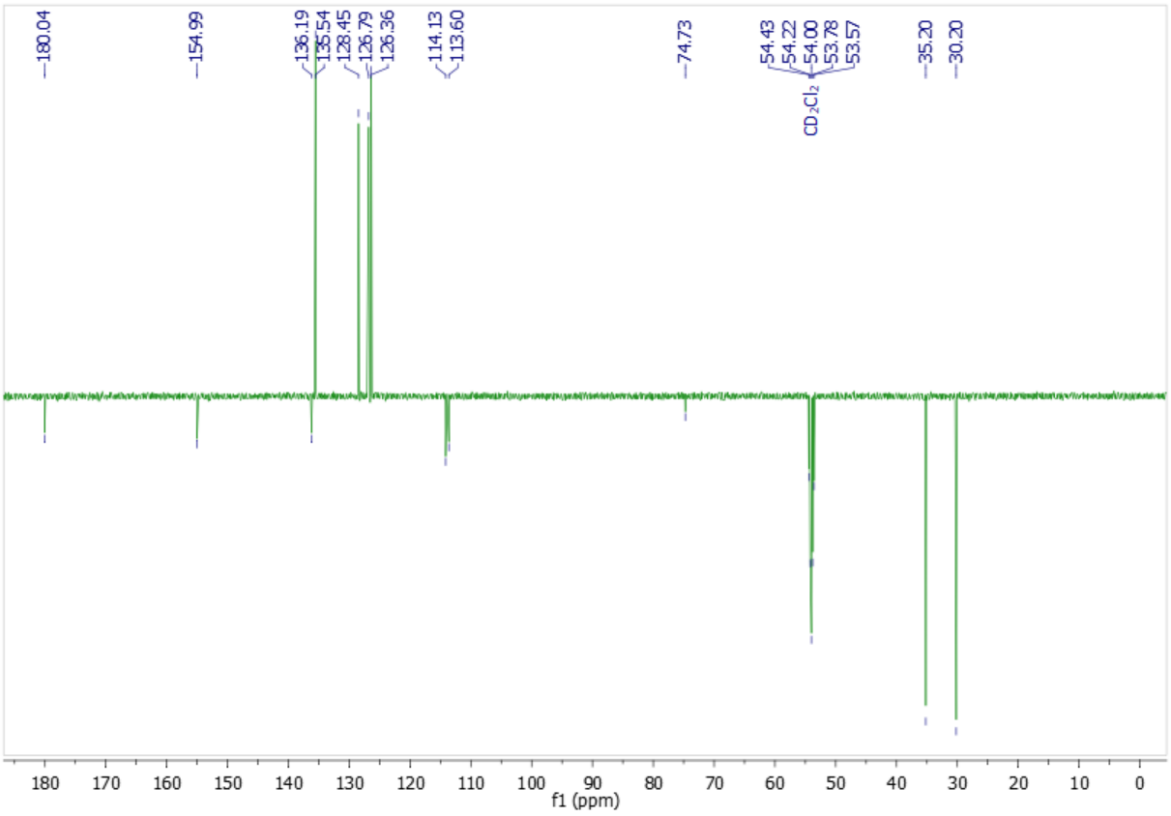

S3.4 ^{1}H NMR of 2-(3-oxo-2,3-dihydro-1*H*-inden-1-ylidene)malononitrile (IDO)

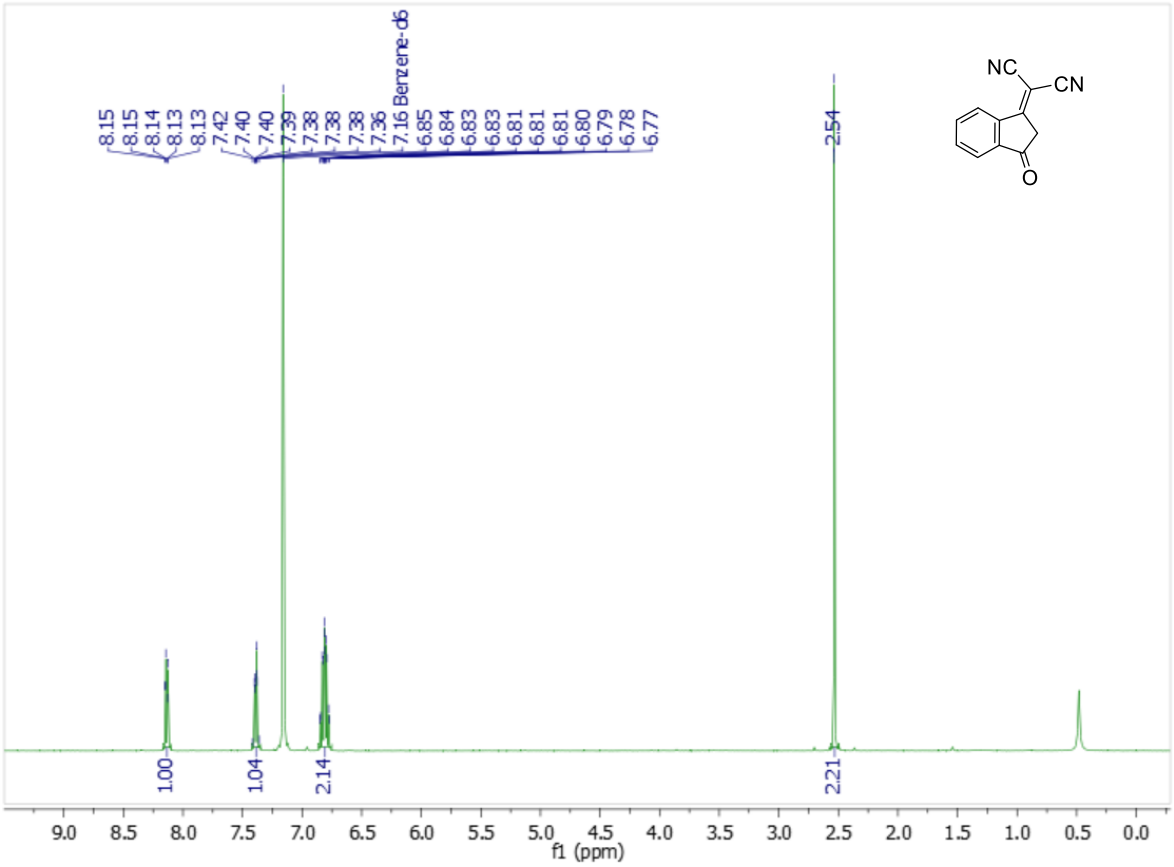

^{13}C NMR of 2-(3-oxo-2,3-dihydro-1*H*-inden-1-ylidene)malononitrile (IDO)

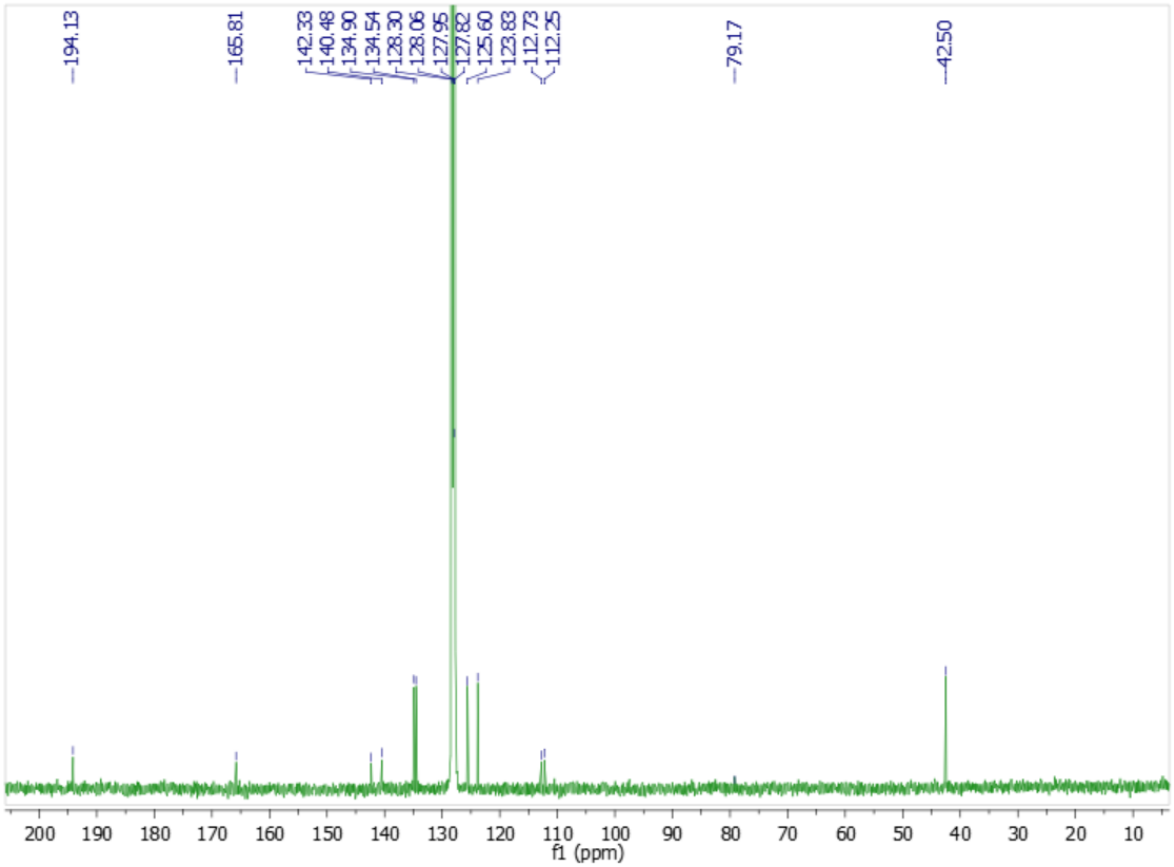

S3.5 ^{1}H NMR of 2-(3-oxo-2,3-dihydro-1*H*-inden-1-ylidene)malononitrile (IDD)

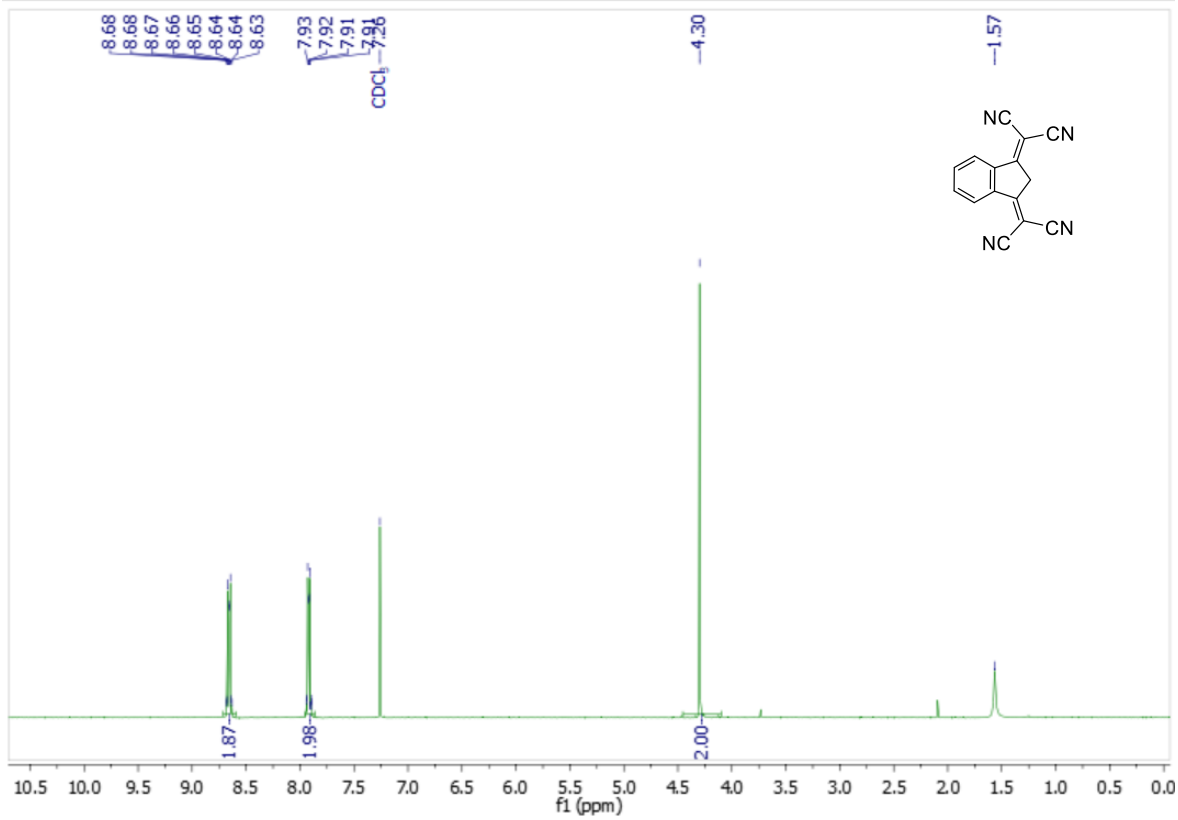

^{13}C NMR of 2-(3-oxo-2,3-dihydro-1*H*-inden-1-ylidene)malononitrile (IDD)

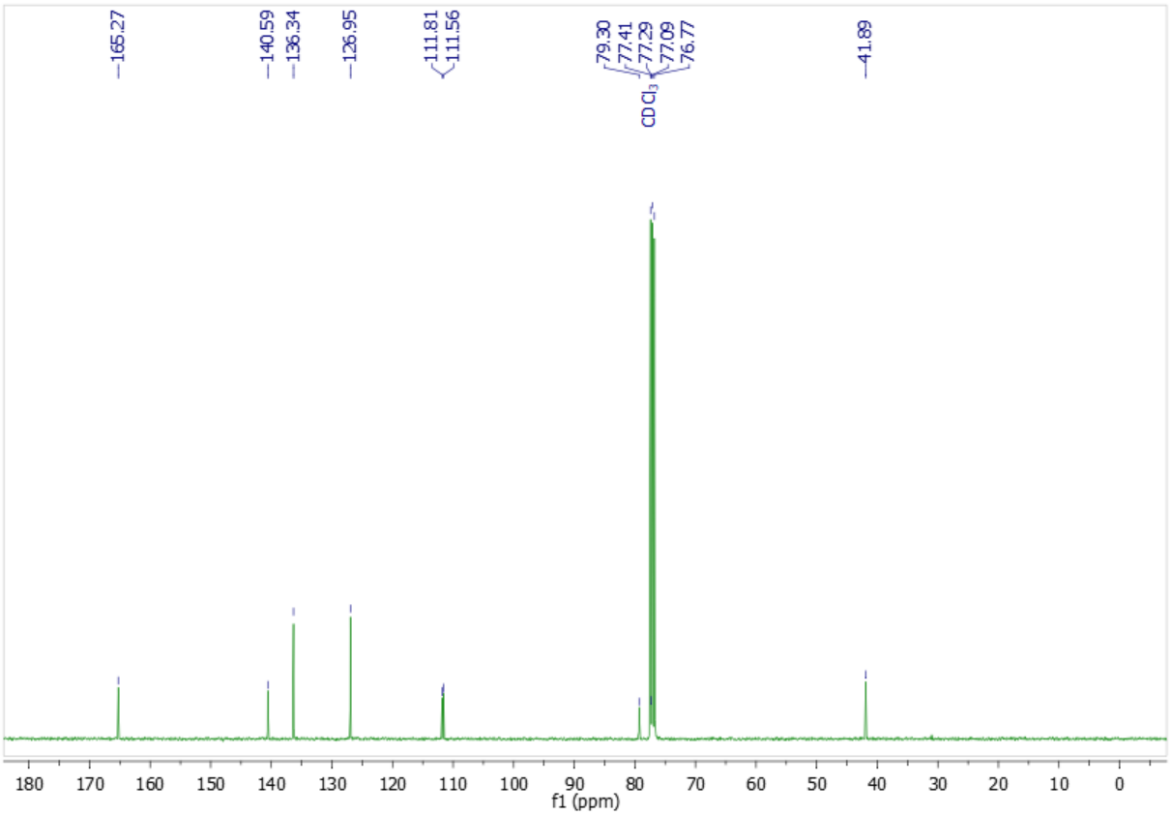

S3.6 ^{1}H NMR of DPPZ-CHO

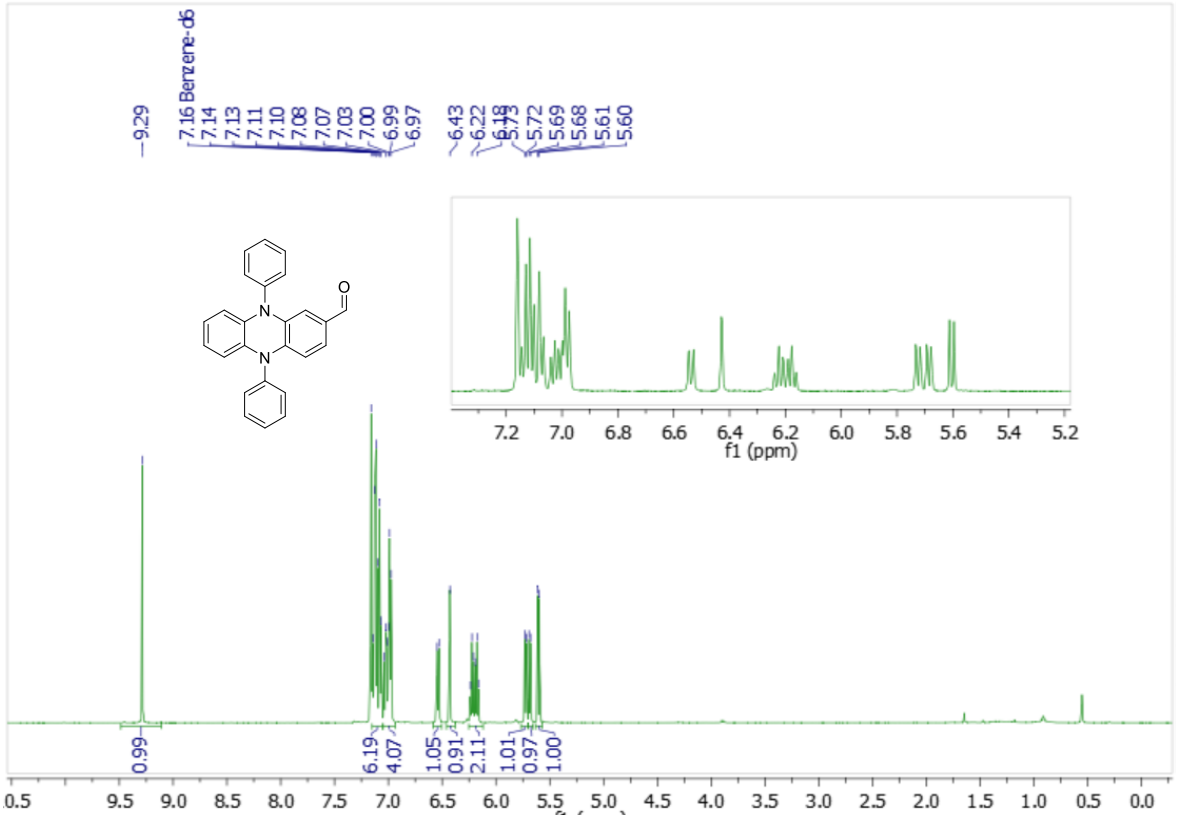

^{13}C NMR of DPPZ-CHO

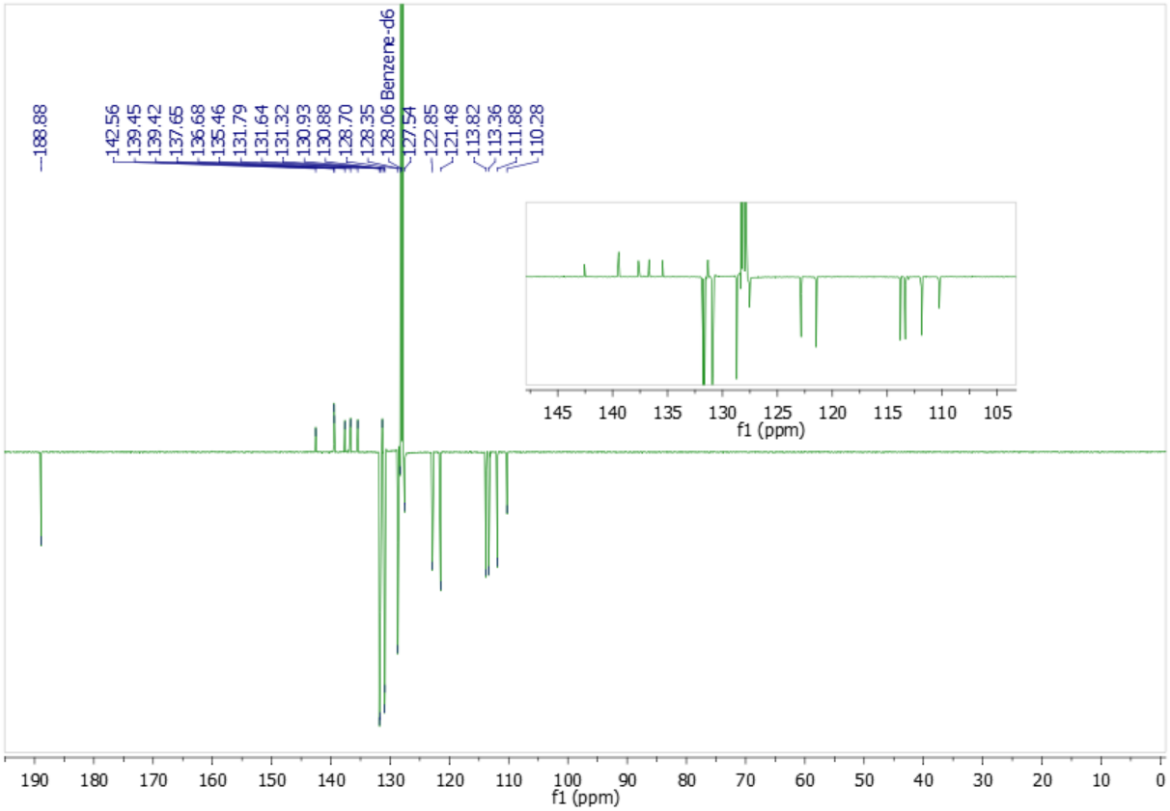

S3.7 ^{1}H NMR of DPPZ-IO

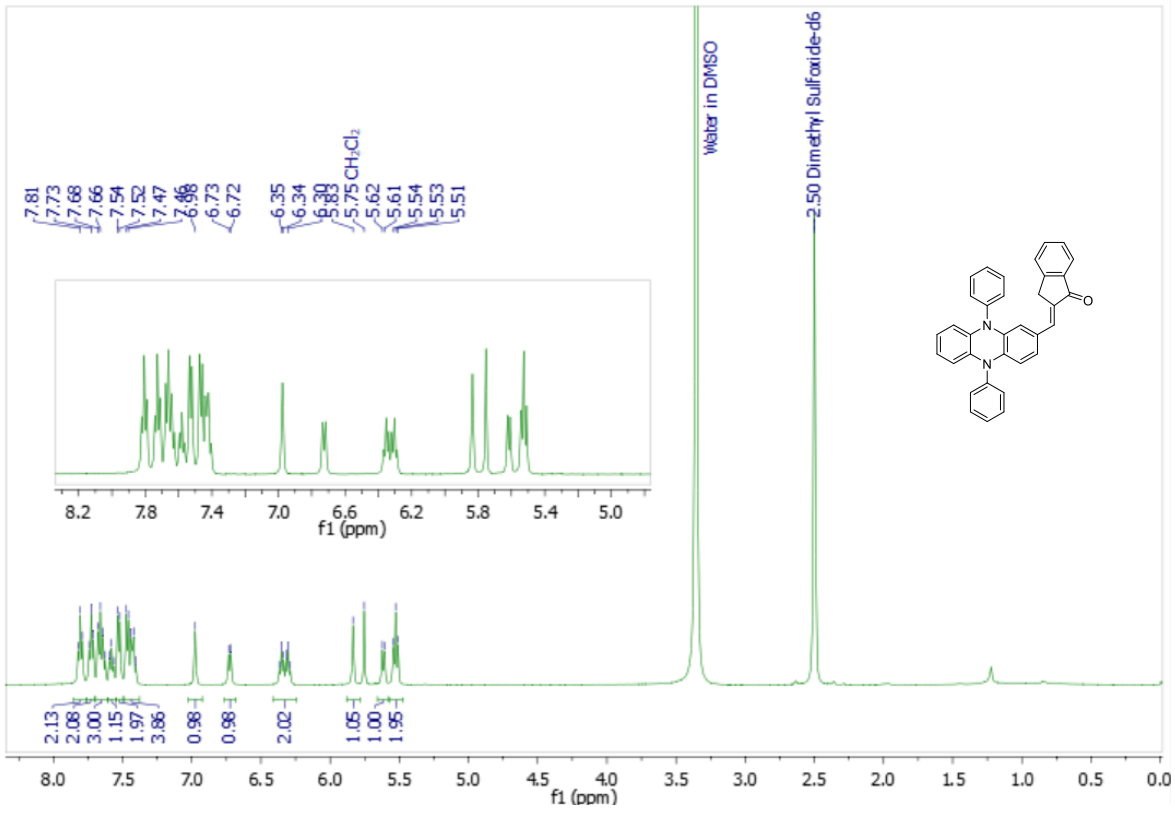

^{13}C NMR of DPPZ-IO

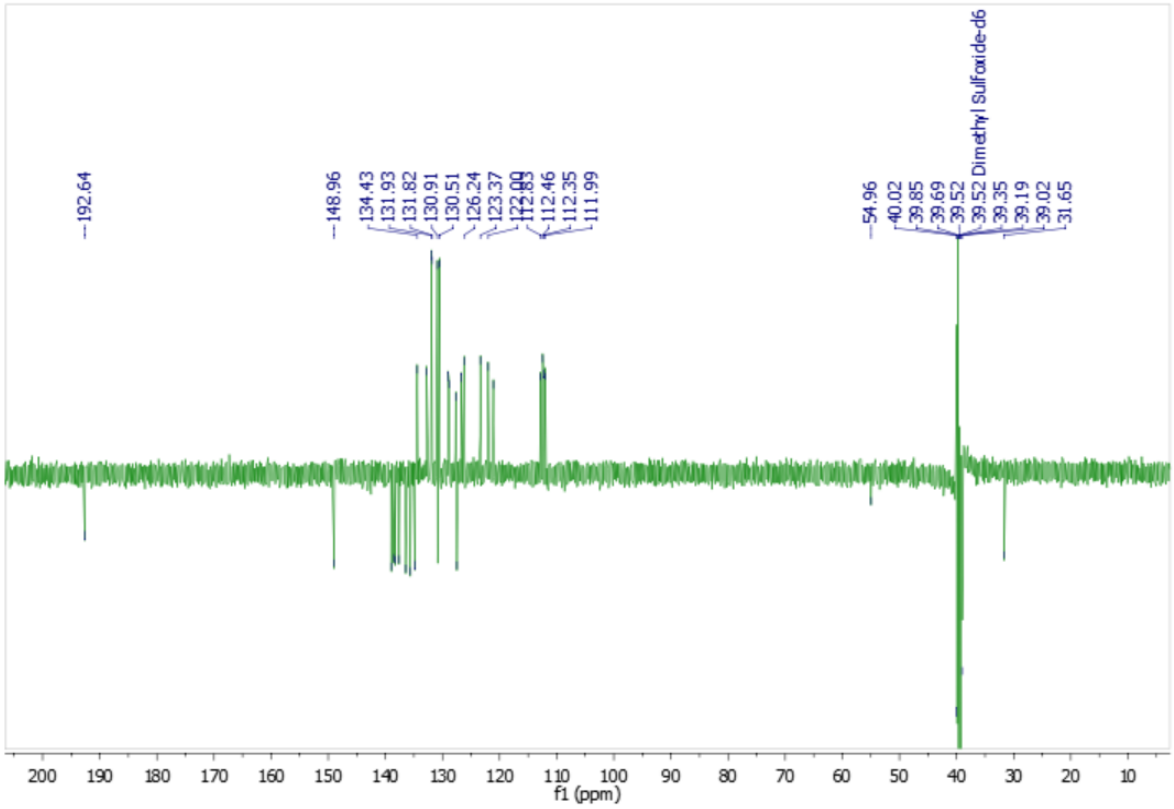

S3.8 ^{1}H NMR of DPPZ-DCV

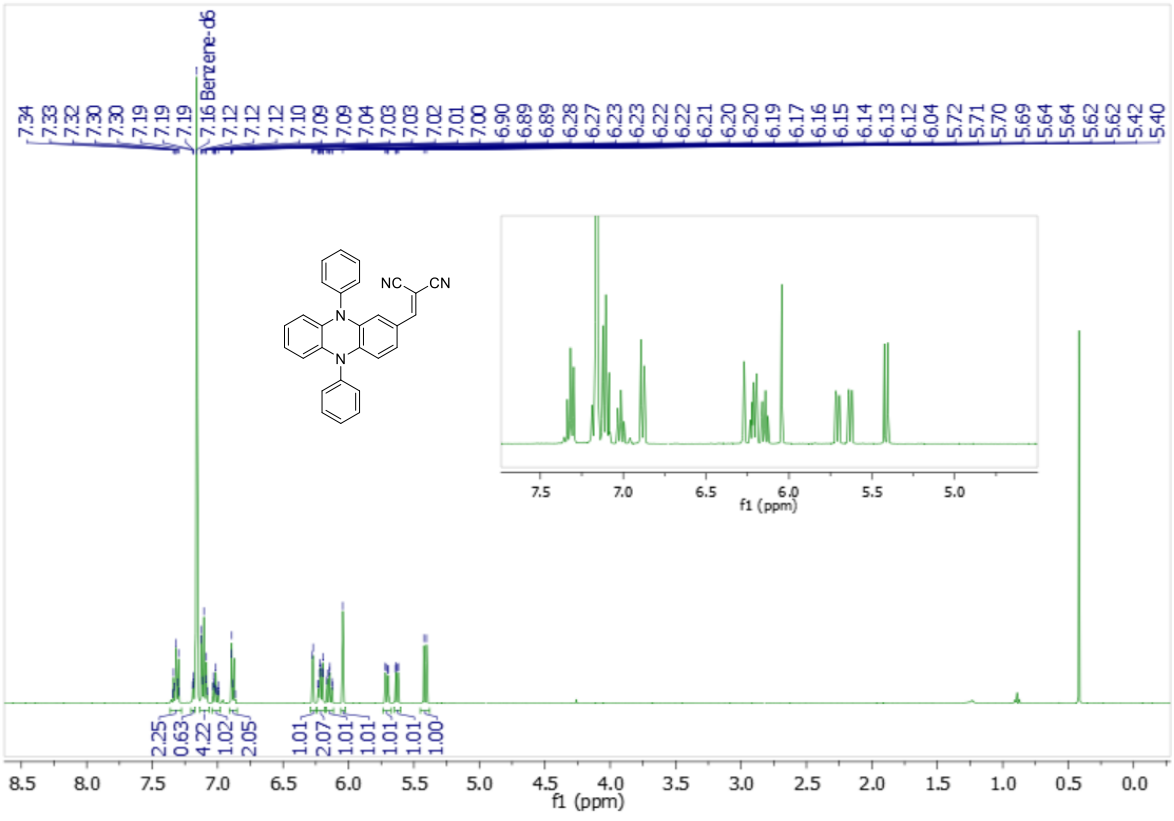

^{13}C NMR of DPPZ-DCV

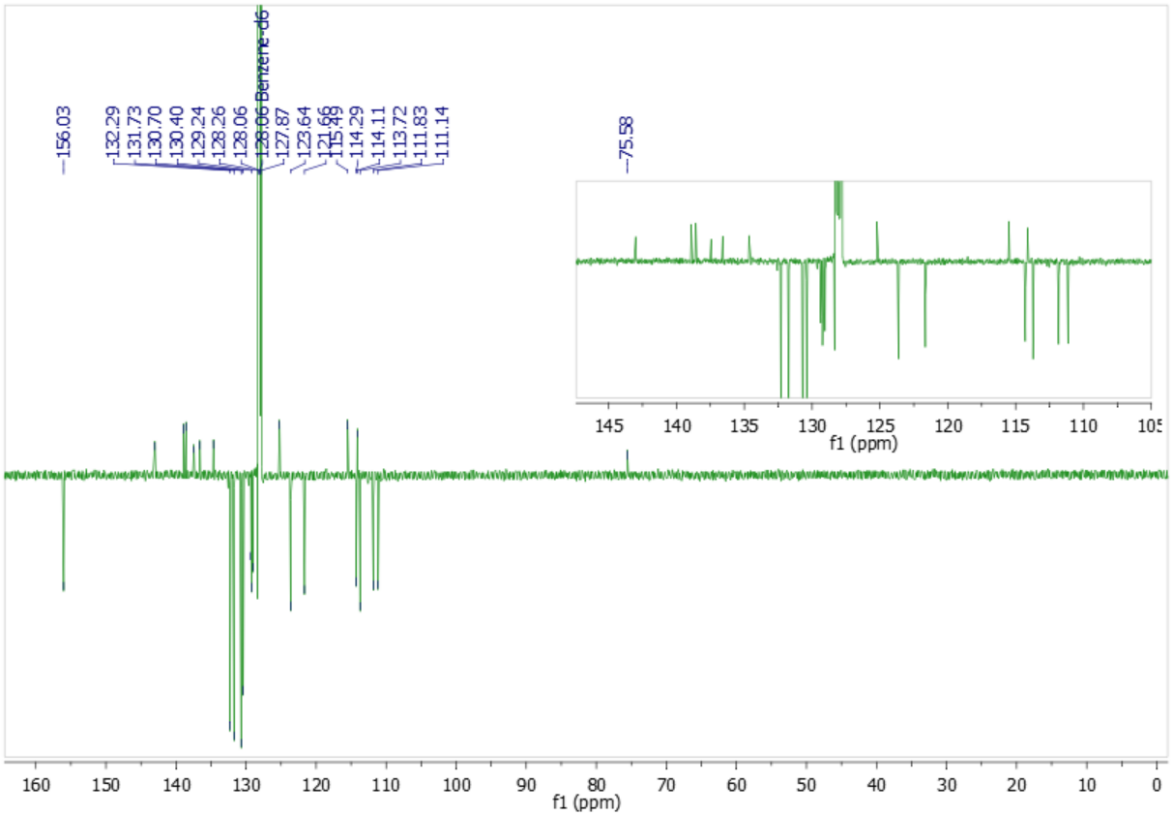

S3.9 ^{1}H NMR of DPPZ-IOO

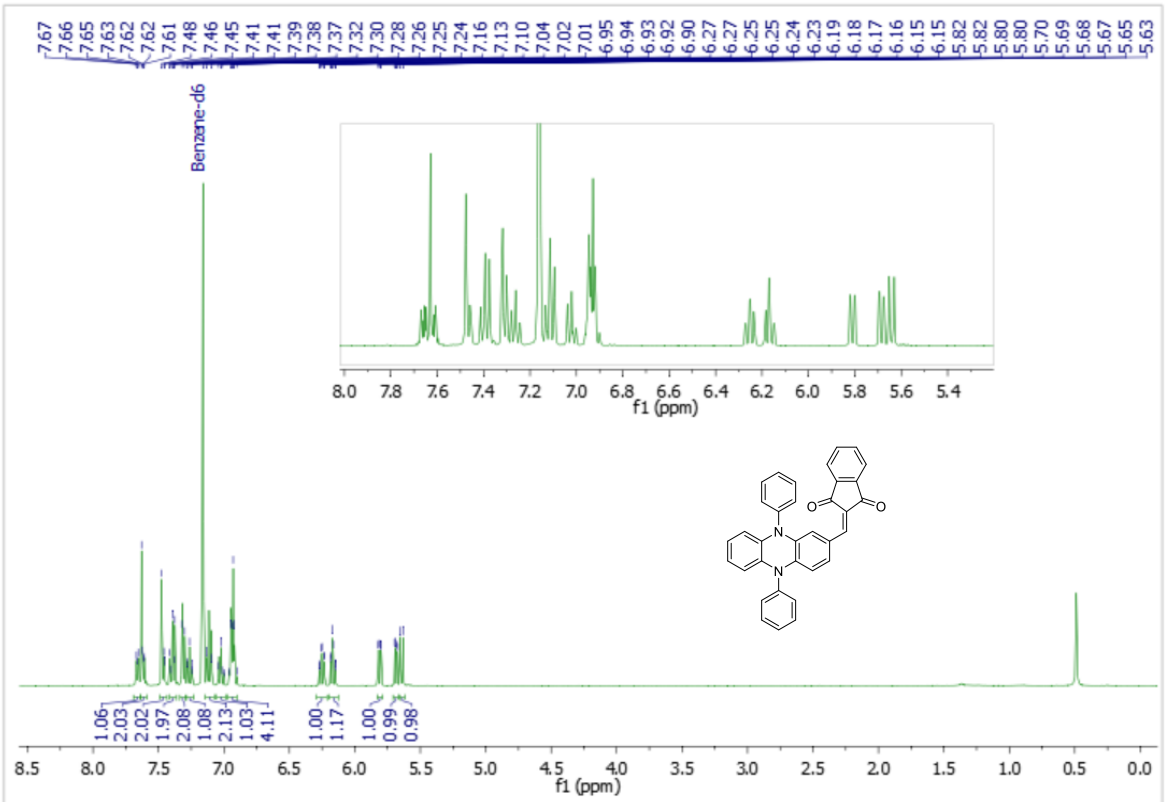

^{13}C NMR of DPPZ-IOO

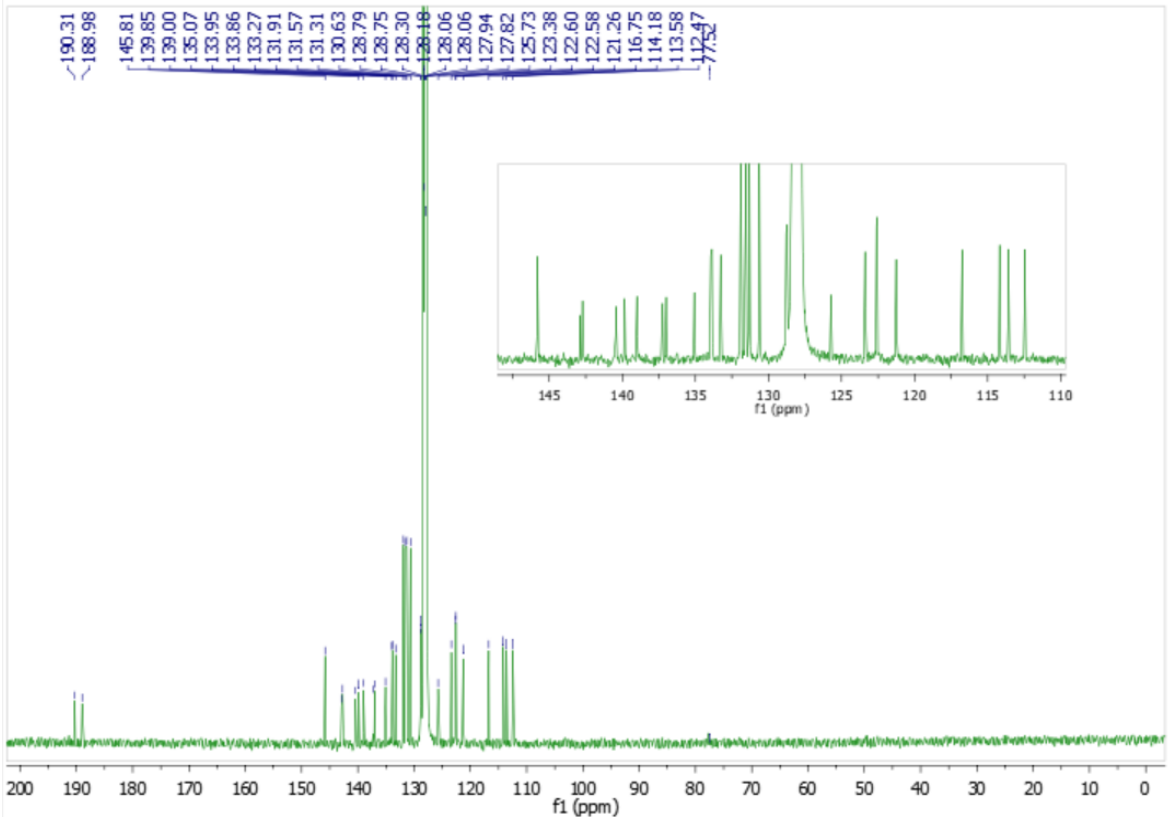

S3.10 ^{1}H NMR of DPPZ-ID

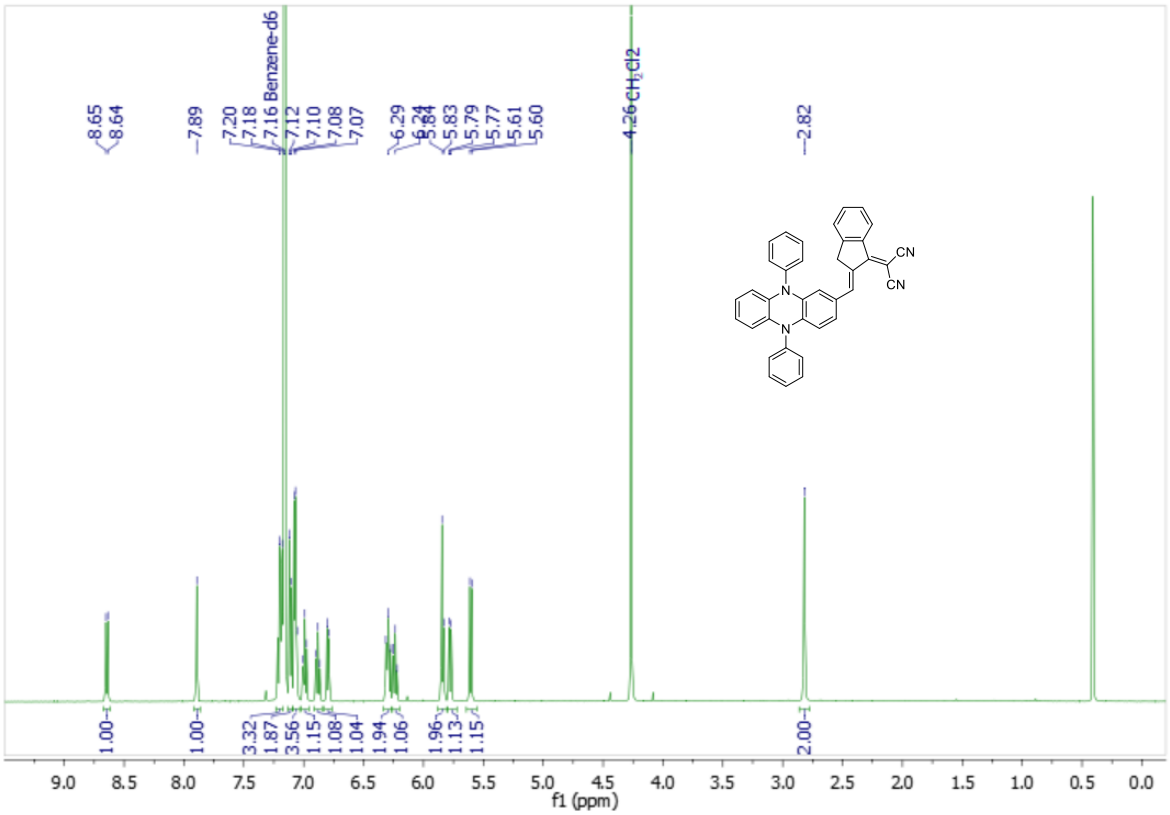

^{13}C NMR of DPPZ-ID

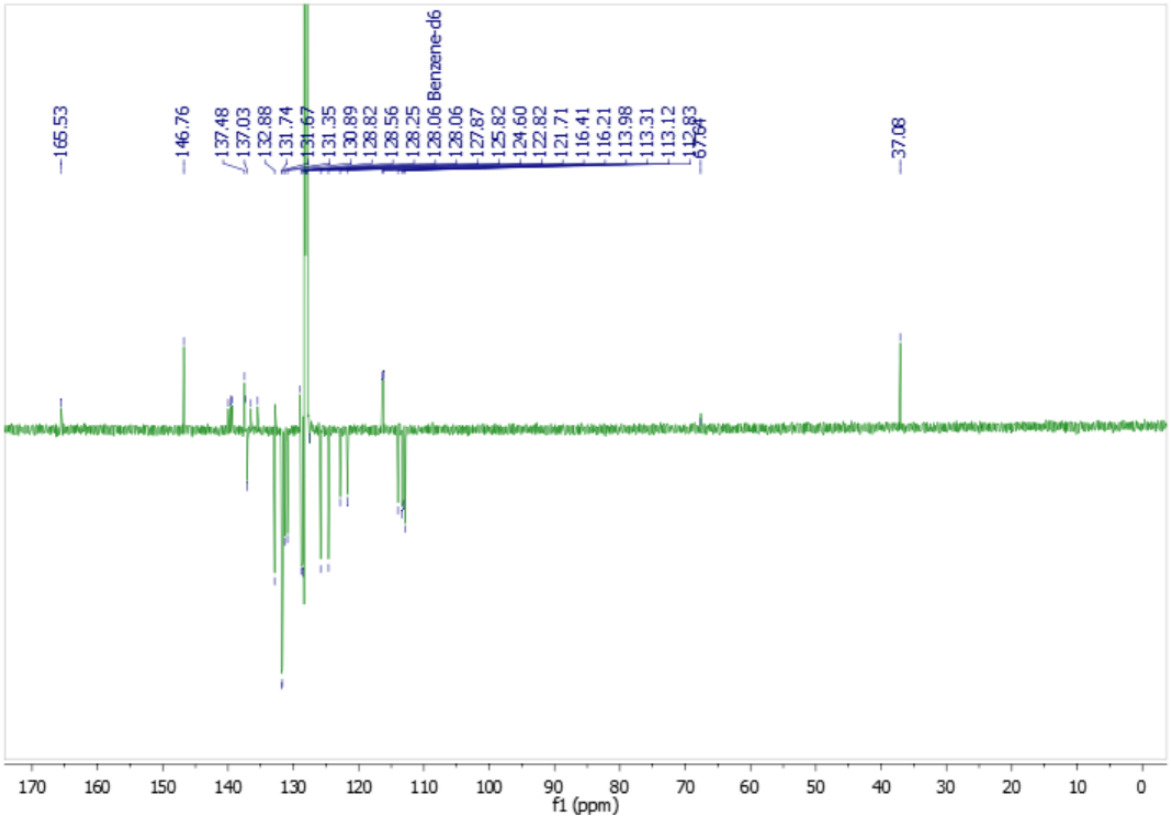

S3.11 ^{1}H NMR of DPPZ-IDO

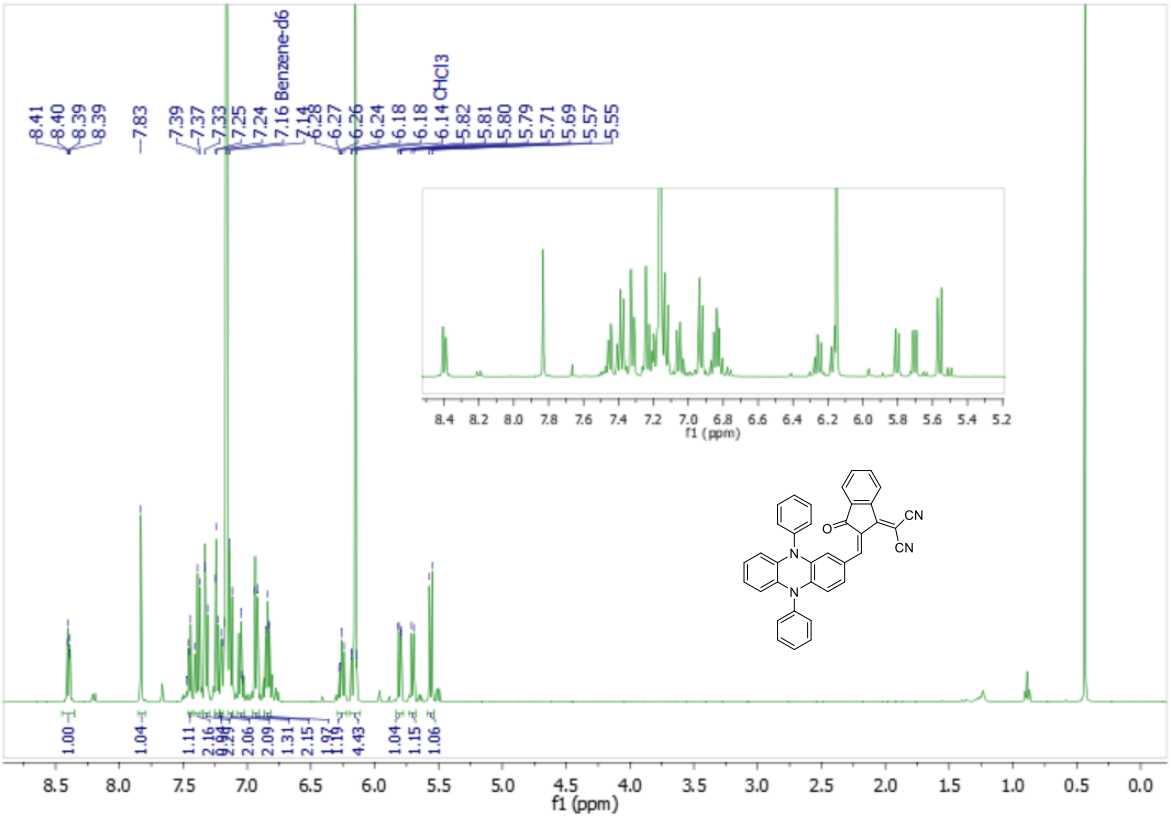

^{13}C NMR of DPPZ-IDO

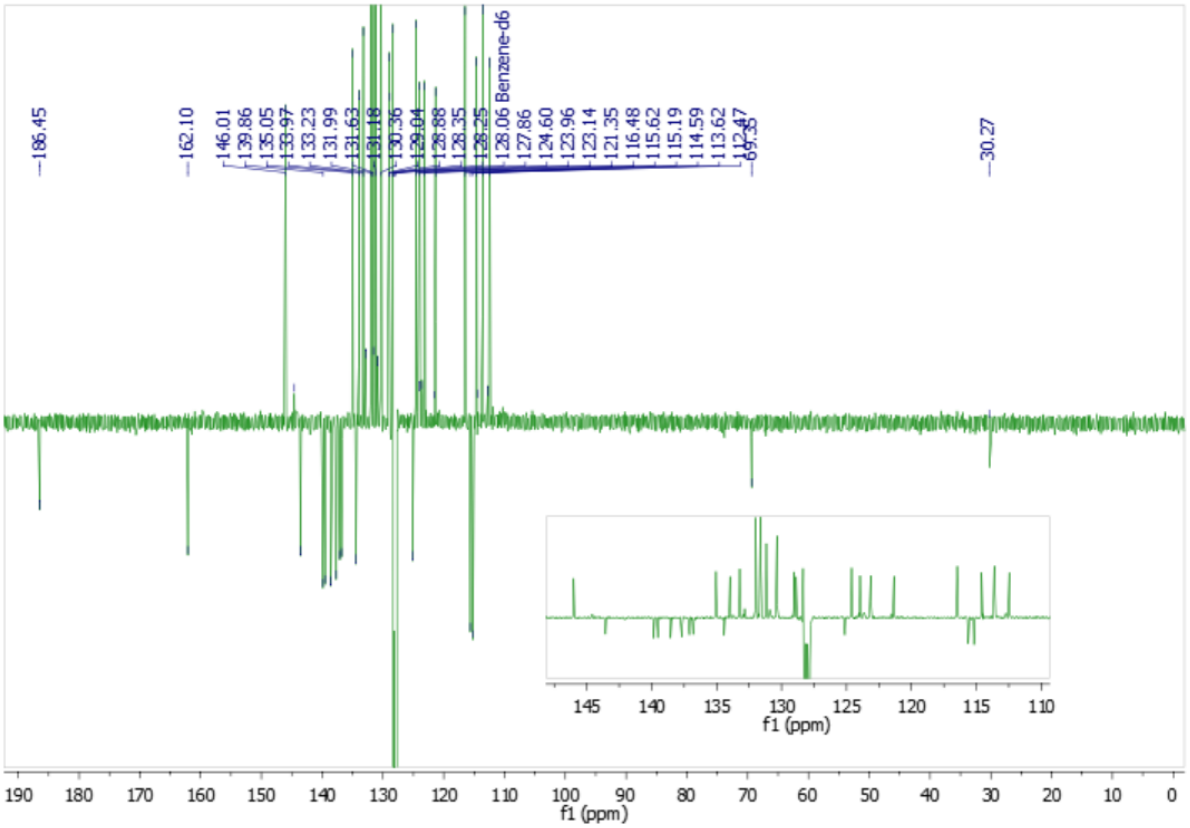

S3.12 ^{1}H NMR of DPPZ-IDD

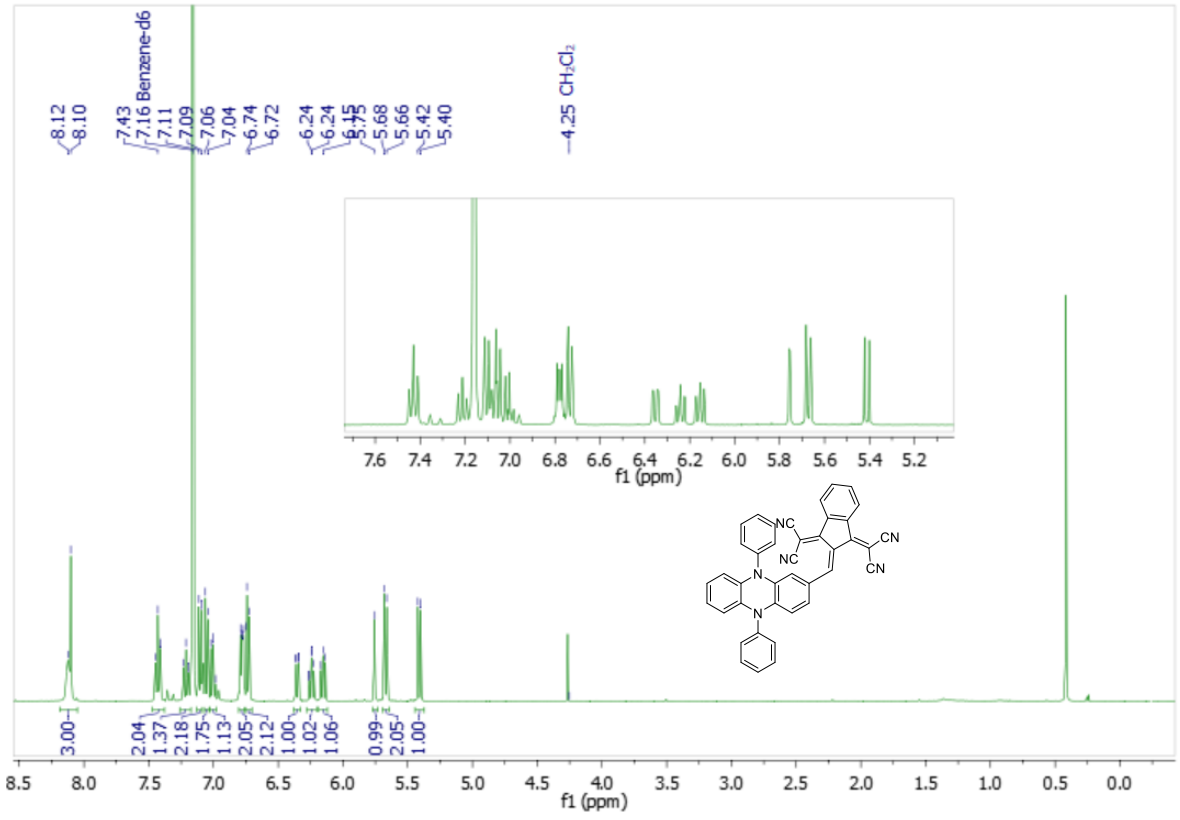

^{13}C NMR of DPPZ-IDD

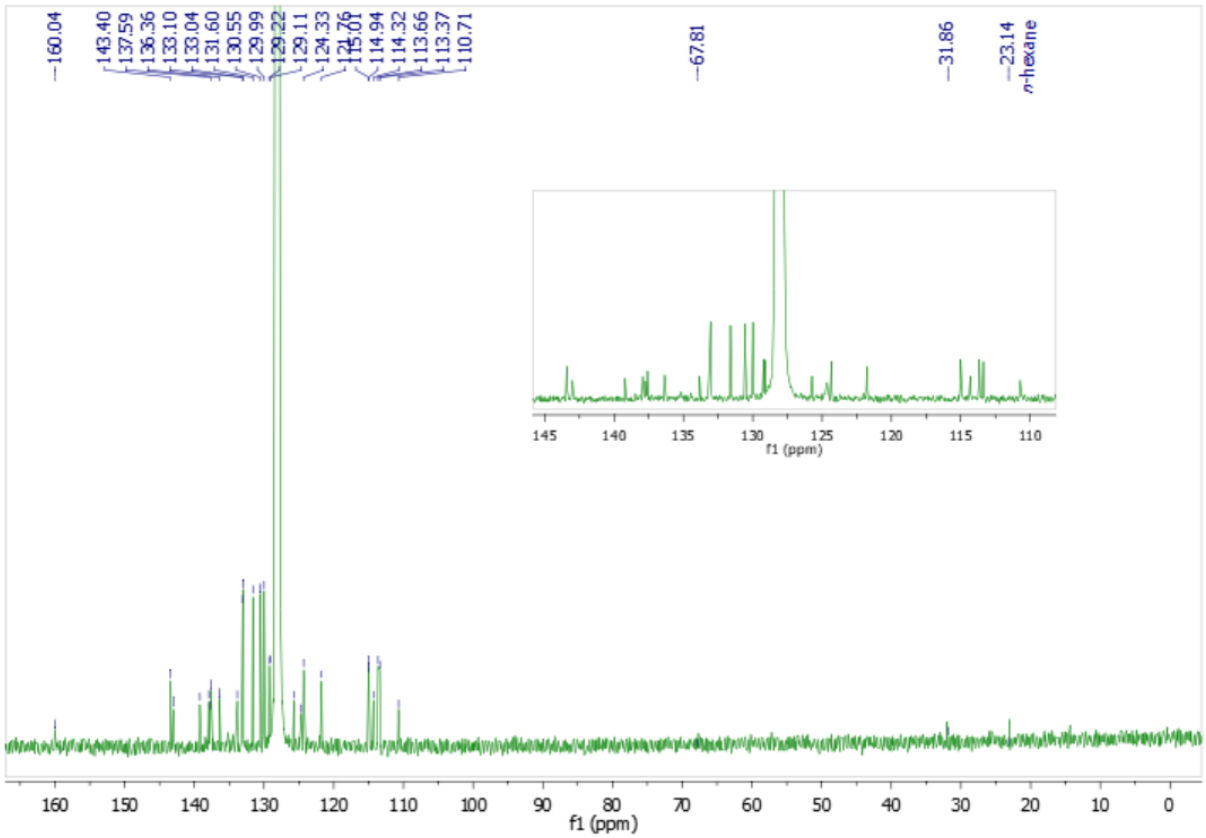

S4 Single crystals

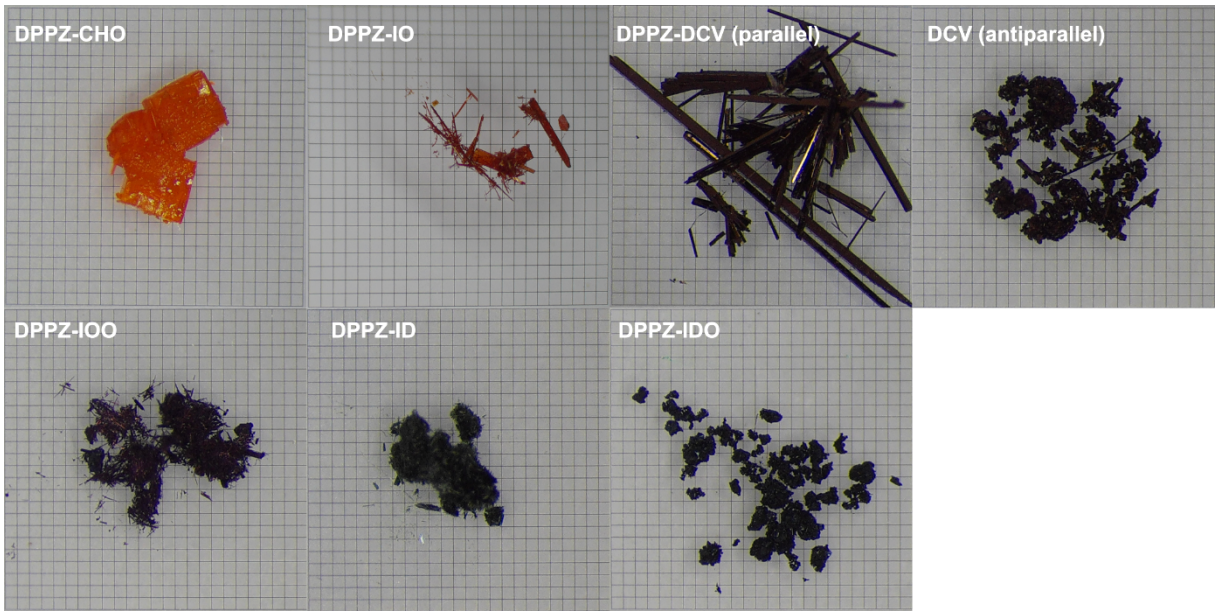

***Figure S1**: Photos of investigated crystals under optical microscope. 1 square = 0.2 mm.*

Table S1: *Experimental details for* ***DPPZ-CHO****.*

Crystal data	
Chemical formula	$C_{25}H_{18}N_2O$
M_r	362.41
Crystal system, space group	Monoclinic, $P2_1$
Temperature (K)	150
a, b, c (Å)	8.6303(5), 9.3503(5), 11.2033(9)
β (°)	96.044(3)
V (Å^3)	899.04(10)
Z	2
Radiation type	Mo $K\alpha$
μ (mm^{-1})	0.08
Crystal size (mm)	0.31 × 0.20 × 0.12
Data collection	
Diffractometer	Bruker D8 - Venture
Absorption correction	Multi-scan *SADABS2016*/2 - Bruker AXS area detector scaling and absorption correction reference [S5].
T_{min}, T_{max}	0.687, 0.746
No. of measured, independent and observed [$I > 2\sigma(I)$] reflections	32565, 4509, 3130
R_{int}	0.087
(sin $\theta/\lambda)_{max}$ (Å^{-1})	0.671
Refinement	
$R[F^2 > 2\sigma(F^2)]$, $wR(F^2)$, S	0.047, 0.138, 1.11
No. of reflections	4509
No. of parameters	453
No. of restraints	463
H-atom treatment	H-atom parameters constrained
$\Delta\rho_{max}$, $\Delta\rho_{min}$ (e Å^{-3})	0.15, −0.17
Absolute structure	Refined as an inversion twin.

Computer programs: Bruker Instrument Service vV6.2.3, *APEX4* v2022.10-0 (Bruker AXS), *SAINT* V8.37A (Bruker AXS Inc., 2015), XT, VERSION 2014/5, *SHELXL2019*/1 (Sheldrick, 2019), *PLATON* (Spek, 2009).

Table S2: *Experimental details for* ***DPPZ-IO****.*

Crystal data	
Chemical formula	$C_{34}H_{24}N_2O \cdot CHCl_3$
M_r	595.92
Crystal system, space group	Triclinic, *P*-1
Temperature (K)	150
a, *b*, *c* (Å)	8.1469(3), 9.8157(3), 19.9241(7)
α, β, γ (°)	100.331(1), 95.032(1), 111.581(1)
V (Å^3)	1436.86(9)
Z	2
Radiation type	Mo *Kα*
μ (mm^{-1})	0.35
Crystal size (mm)	0.38 × 0.12 × 0.02
Data collection	
Diffractometer	Bruker D8 - Venture
Absorption correction	Multi-scan *SADABS2016*/2 - Bruker AXS area detector scaling and absorption correction
T_{min}, T_{max}	0.718, 0.746
No. of measured, independent and observed [$I > 2\sigma(I)$] reflections	95127, 7148, 5330
R_{int}	0.074
(sin $\theta/\lambda)_{max}$ (Å^{-1})	0.668
Refinement	
$R[F^2 > 2\sigma(F^2)]$, $wR(F^2)$, S	0.043, 0.124, 1.03
No. of reflections	7148
No. of parameters	398
No. of restraints	345
H-atom treatment	H-atom parameters constrained
$\Delta\rho_{max}$, $\Delta\rho_{min}$ (e Å^{-3})	0.32, −0.43

Computer programs: Bruker Instrument Service vV6.2.3, *APEX4* v2022.10-0 (Bruker AXS), *SAINT* V8.37A (Bruker AXS Inc., 2015), XT, VERSION 2014/5, *SHELXL2019*/1 (Sheldrick, 2019), *PLATON* (Spek, 2009).

Table S3: *Experimental details for* ***DPPZ-DCV*** *(parallel).*

Crystal data	
Chemical formula	$C_{28}H_{18}N_4 \cdot 0.5(CHCl_3)$
M_r	470.15
Crystal system, space group	Monoclinic, $P2_1/n$
Temperature (K)	150
a, b, c (Å)	5.6839(3), 29.8005(19), 13.5748(9)
β (°)	93.709(2)
V (Å^3)	2294.5(2)
Z	4
Radiation type	Mo $K\alpha$
μ (mm^{-1})	0.25
Crystal size (mm)	0.40 × 0.18 × 0.02
Data collection	
Diffractometer	Bruker D8 - Venture
Absorption correction	Multi-scan *SADABS2016*/2 - Bruker AXS area detector scaling and absorption correction
T_{min}, T_{max}	0.679, 0.746
No. of measured, independent and observed [$I > 2\sigma(I)$] reflections	65499, 4485, 3425
R_{int}	0.113
(sin $\theta/\lambda)_{max}$ (Å^{-1})	0.617
Refinement	
$R[F^2 > 2\sigma(F^2)]$, $wR(F^2)$, S	0.047, 0.119, 1.01
No. of reflections	4485
No. of parameters	290
No. of restraints	258
H-atom treatment	H-atom parameters constrained
$\Delta\rho_{max}$, $\Delta\rho_{min}$ (e Å^{-3})	0.28, −0.17

Computer programs: Bruker Instrument Service vV6.2.3, *APEX4* v2022.10-0 (Bruker AXS), *SAINT* V8.37A (Bruker AXS Inc., 2015), XT, VERSION 2014/5, *SHELXL2019*/1 (Sheldrick, 2019), *PLATON* (Spek, 2009).

Table S4: *Experimental details for* ***DPPZ-IOO*** *(prism).*

Crystal data	
Chemical formula	$C_{34}H_{22}N_2O_2 \cdot CHCl_3$
M_r	609.90
Crystal system, space group	Monoclinic, $P2_1/c$
Temperature (K)	150
a, b, c (Å)	11.6294(5), 10.6677(5), 23.0449(11)
β (°)	92.494(2)
V (Å^3)	2856.2(2)
Z	4
Radiation type	Mo $K\alpha$
μ (mm^{-1})	0.36
Crystal size (mm)	0.36 × 0.19 × 0.14
Data collection	
Diffractometer	Bruker D8 - Venture
Absorption correction	Multi-scan *SADABS2016*/2 - Bruker AXS area detector scaling and absorption correction reference [S5]
T_{min}, T_{max}	0.706, 0.746
No. of measured, independent and observed [$I > 2\sigma(I)$] reflections	84646, 7096, 5724
R_{int}	0.074
(sin $\theta/\lambda)_{max}$ (Å^{-1})	0.667
Refinement	
$R[F^2 > 2\sigma(F^2)]$, $wR(F^2)$, S	0.045, 0.121, 1.04
No. of reflections	7096
No. of parameters	407
No. of restraints	366
H-atom treatment	H-atom parameters constrained
$\Delta\rho_{max}$, $\Delta\rho_{min}$ (e Å^{-3})	0.41, −0.50

Computer programs: Bruker Instrument Service vV6.2.3, *APEX4* v2022.10-0 (Bruker AXS), *SAINT* V8.37A (Bruker AXS Inc., 2015), XT, VERSION 2014/5, *SHELXL2019*/1 (Sheldrick, 2019), *PLATON* (Spek, 2009).

Table S5: *Experimental details for* ***DPPZ-IOO*** *(needle).*

Crystal data	
Chemical formula	$C_{34}H_{22}N_2O_2 \cdot CHCl_3$
M_r	609.90
Crystal system, space group	Triclinic, *P*-1
Temperature (K)	150
a, *b*, *c* (Å)	8.125(3), 9.774(3), 19.278(6)
α, β, γ (°)	101.044(15), 94.908(15), 111.203(13)
V (Å^3)	1380.6(8)
Z	2
Radiation type	Mo *Kα*
μ (mm^{-1})	0.37
Crystal size (mm)	0.25 × 0.04 × 0.03
Data collection	
Diffractometer	Bruker D8 - Venture
Absorption correction	Multi-scan *SADABS2016*/2 - Bruker AXS area detector scaling and absorption correction reference [S5]
T_{min}, T_{max}	0.514, 0.745
No. of measured, independent and observed [$I > 2\sigma(I)$] reflections	36910, 4952, 3276
R_{int}	0.151
(sin $\theta/\lambda)_{max}$ (Å^{-1})	0.606
Refinement	
$R[F^2 > 2\sigma(F^2)]$, $wR(F^2)$, S	0.125, 0.332, 1.04
No. of reflections	4952
No. of parameters	379
No. of restraints	339
H-atom treatment	H-atom parameters constrained
$\Delta\rho_{max}$, $\Delta\rho_{min}$ (e Å^{-3})	0.69, −0.67

Computer programs: *SHELXL2019*/1 (Sheldrick, 2019).

Table S6: *Experimental details for* ***DPPZ-ID****.*

Crystal data	
Chemical formula	$C_{37}H_{24}N_4$
M_r	524.60
Crystal system, space group	Triclinic, *P*-1
Temperature (K)	150
a, *b*, *c* (Å)	9.0974(5), 11.2035(7), 13.7565(8)
α, β, γ (°)	104.932(2), 96.023(2), 90.760(2)
V (Å^3)	1346.09(14)
Z	2
Radiation type	Mo *Kα*
μ (mm^{-1})	0.08
Crystal size (mm)	0.39 × 0.09 × 0.03
Data collection	
Diffractometer	Bruker D8 - Venture
Absorption correction	Multi-scan *SADABS2016*/2 - Bruker AXS area detector scaling and absorption correction
T_{min}, T_{max}	0.567, 0.745
No. of measured, independent and observed [$I > 2\sigma(I)$] reflections	36198, 5447, 3374
R_{int}	0.107
(sin $\theta/\lambda)_{max}$ (Å^{-1})	0.626
Refinement	
$R[F^2 > 2\sigma(F^2)]$, $wR(F^2)$, S	0.063, 0.166, 1.05
No. of reflections	5447
No. of parameters	370
No. of restraints	342
H-atom treatment	H-atom parameters constrained
$\Delta\rho_{max}$, $\Delta\rho_{min}$ (e Å^{-3})	0.21, −0.22

Computer programs: Bruker Instrument Service vV6.2.3, *APEX4* v2022.10-0 (Bruker AXS), *SAINT* V8.37A (Bruker AXS Inc., 2015), XT, VERSION 2014/5, *SHELXL2019*/1 (Sheldrick, 2019), *PLATON* (Spek, 2009).

Table S7: *Experimental details for* ***DPPZ-IDO****.*

Crystal data	
Chemical formula	$C_{37}H_{22}N_4O$
M_r	538.58
Crystal system, space group	Triclinic, *P*-1
Temperature (K)	150
a, *b*, *c* (Å)	7.4903(5), 10.6162(6), 17.7475(11)
α, β, γ (°)	93.111(2), 100.842(3), 104.567(2)
V (Å^3)	1333.83(14)
Z	2
Radiation type	Mo *Kα*
μ (mm^{-1})	0.08
Crystal size (mm)	0.15 × 0.14 × 0.03
Data collection	
Diffractometer	Bruker D8 - Venture
Absorption correction	Multi-scan *SADABS2016*/2 - Bruker AXS area detector scaling and absorption correction
T_{min}, T_{max}	0.699, 0.742
No. of measured, independent and observed [$I > 2\sigma(I)$] reflections	74077, 5531, 4098
R_{int}	0.116
(sin $\theta/\lambda)_{max}$ (Å^{-1})	0.628
Refinement	
$R[F^2 > 2\sigma(F^2)]$, $wR(F^2)$, S	0.046, 0.117, 0.99
No. of reflections	5531
No. of parameters	380
No. of restraints	351
H-atom treatment	H-atom parameters constrained
$\Delta\rho_{max}$, $\Delta\rho_{min}$ (e Å^{-3})	0.30, −0.23

Computer programs: Bruker Instrument Service vV6.2.3, *APEX4* v2022.10-0 (Bruker AXS), *SAINT* V8.37A (Bruker AXS Inc., 2015), XT, VERSION 2014/5, *SHELXL2019*/1 (Sheldrick, 2019), *PLATON* (Spek, 2009).

S5 Electrochemistry

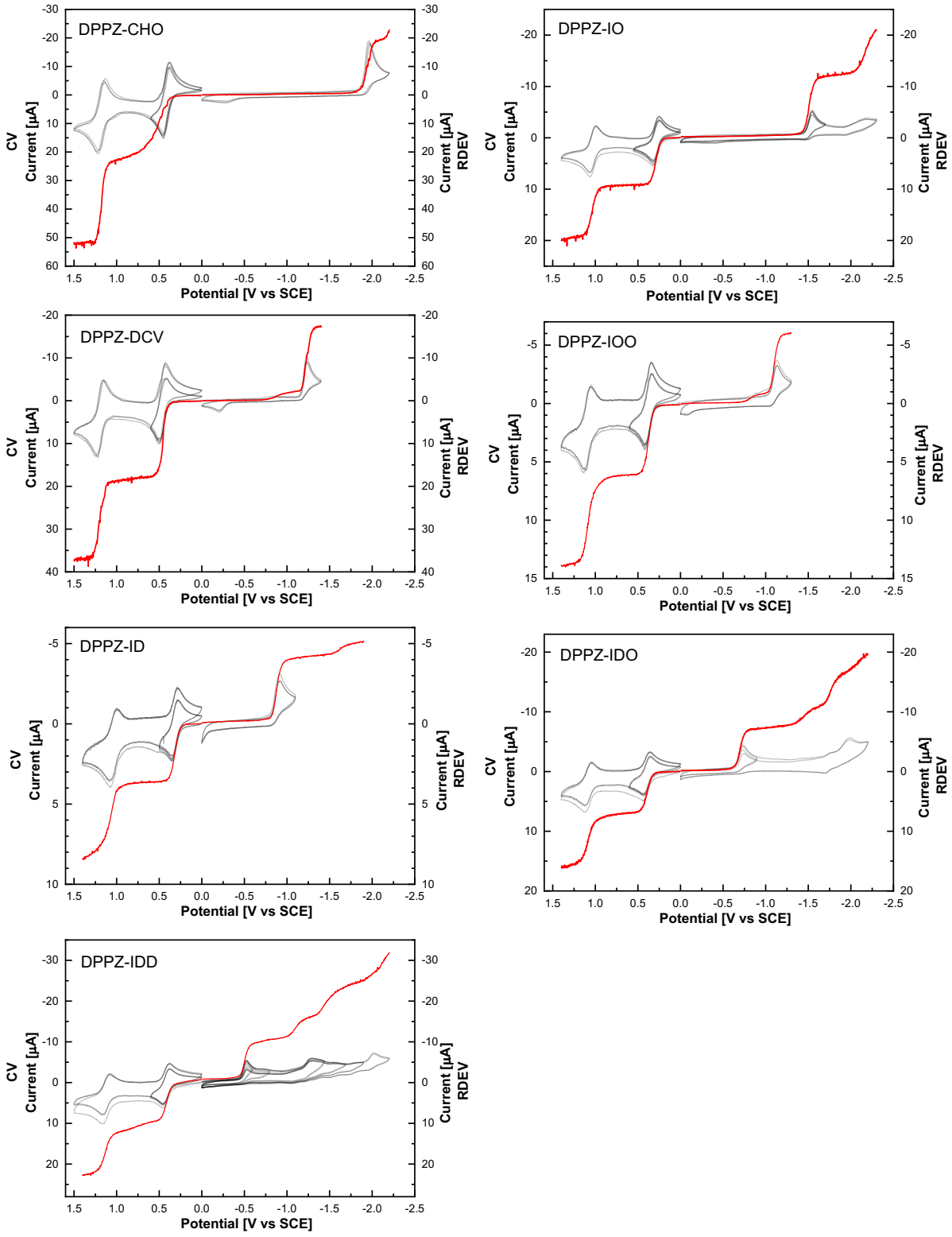

***Figure S2**: Cyclic (CV, grey lines) and rotating disk electrode (RDEV, red lines) voltammograms obtained at glassy carbon electrode in CH_3CN containing 0.1 M Bu_4NPF_6 at the scan rate of 100 mV/s, rotation frequency f = 500 min^{-1}.*

***Table S8**: Summary of HOMO and LUMO energy levels and redox potentials of **DPPZ-EWG**.*

Compounds		Theory			Experiment				
		HOMO[a]	**LUMO**[a]	ΔE	$E_{1/2,\ ox1}$[b]	$E_{1/2,\ red1}$[b]	**HOMO**[c]	**LUMO**[c]	ΔE
DPPZ-CHO	*cis*	-4.590	-2.076	2.51	0.413	-1.941	-4.846	-2.488	2.36
	trans	-4.630	-2.055	2.58					
DPPZ-IO	*cis*	-4.502	-2.598	1.90	0.288	-1.513	-4.707	-2.908	1.80
	trans	-4.521	-2.580	1.94					
DPPZ-DCV	*cis*	-4.741	-2.972	1.75	0.454	-1.226	-4.883	-3.203	1.68
	trans	-4.783	-2.931	1.85					
DPPZ-IOO	*cis*	-4.634	-2.989	1.65	0.366	-1.099	-4.795	-3.330	1.47
	trans	-4.649	-2.967	1.68					
DPPZ-ID	*cis*	-4.595	-3.318	1.28	0.315	-0.898	-4.744	-3.531	1.21
	trans	-4.616	-3.298	1.32					
DPPZ-IDO	*cis*	-4.714	-3.444	1.27	0.393	-0.703	-4.822	-3.726	1.10
	trans	-4.725	-3.427	1.30					
DPPZ-IDD	*cis*	-4.716	-3.707	1.01	0.415	-0.513	-4.844	-3.916	0.93
	trans	-4.767	-3.679	1.09					

[a]Theoretical HOMO and LUMO levels were obtained as the difference between adiabatic energies, computed by DFT: PCM B3LYP 6-311G(d,p) by an optimization of S_0, radical cation and radical anion in CH_3CN. [b]All obtained potentials [V] are given vs. SCE. [c]HOMO and LUMO energies were computed from the first oxidation and reduction potentials respectively, according to formula $-E_{HOMO\ or\ LUMO}$ [eV] = $E_{1/2,\ (ox1\ or\ red1)}$ + 4.429 [S9].

S6 DFT calculations

TD-DFT calculations of Frack-Condon geometry

CAM-B3LYP computed excitation energies are considerably higher than those of B3LYP and the experiments, but the CAM correction can give overall more consistent results within the whole set, and rectify the spurious predictions of B3LYP excitation energies and intensities for the transitions with varying charge transfer extent [S6]. There are relevant physical arguments, why not to use PCM TD DFT methodology for the description of absorption, for which only fast solvation is present [S7]. Especially, B3LYP functional should be avoided due to its characteristic over-polarization error [S8]. However, we consider that an apparent agreement between calculations and experiment allows us at least to characterize the crucial excited states by B3LYP results, so as it was done for the interpretation of electrochemical processes. The relative oscillator strengths of CT_1 and CT_2 transitions evaluated by CAM-B3LYP are more realistic (Figure 8), thus confirming a usefulness of simultaneous use of both xc functionals for the prediction and interpretation of the spectra.

As expected [S6], full electron transfer in CS transition recalls considerably bigger difference between B3LYP and CAM-B3LYP transition energies (always higher than 0.9 eV for **DPPZ-IOO**, **DPPZ-IDO** and **DPPZ-IDD** set) as compared to partial charge transfer in CT_1 (always lower than 0.6 eV for the same set) (Table 2). Finally, according to CAM-B3LYP the energy difference between CT_1 and CS states dramatically decreases within this set from 1.13 eV, over 0.79 eV to 0.39 eV, respectively. According to B3LYP calculations, these two states

are even inverted for **DPPZ-IDD** (Table 2). Although a dramatic lowering of the excitation energy of a transition with pronounced charge separation is often considered as spurious [S6, S8], this is not the case of **DPPZ-IDD**.

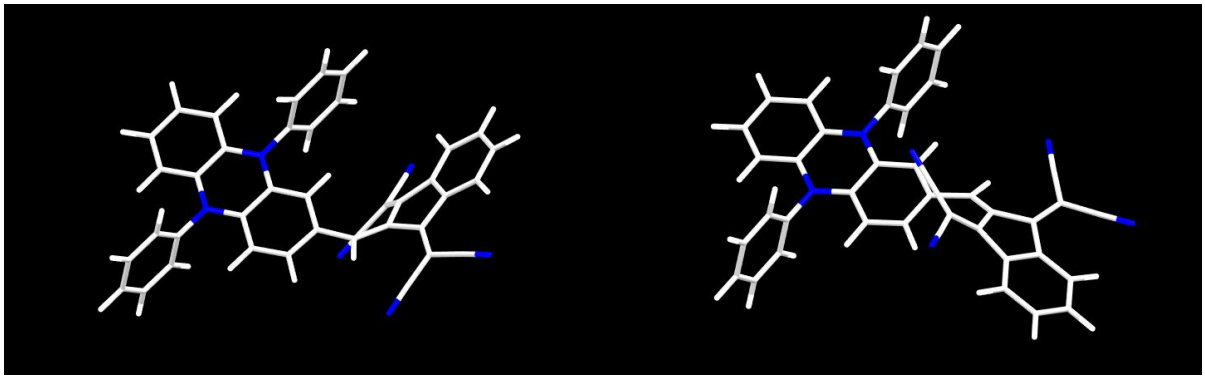

Figure S3*: Optimized geometries of s-cis (left) and s-trans (right) conformers of* ***DPPZ-IDD*** *calculated with DFT at the CAM-B3LYP/6-311G(d,p) with PCM ($CHCl_3$).*

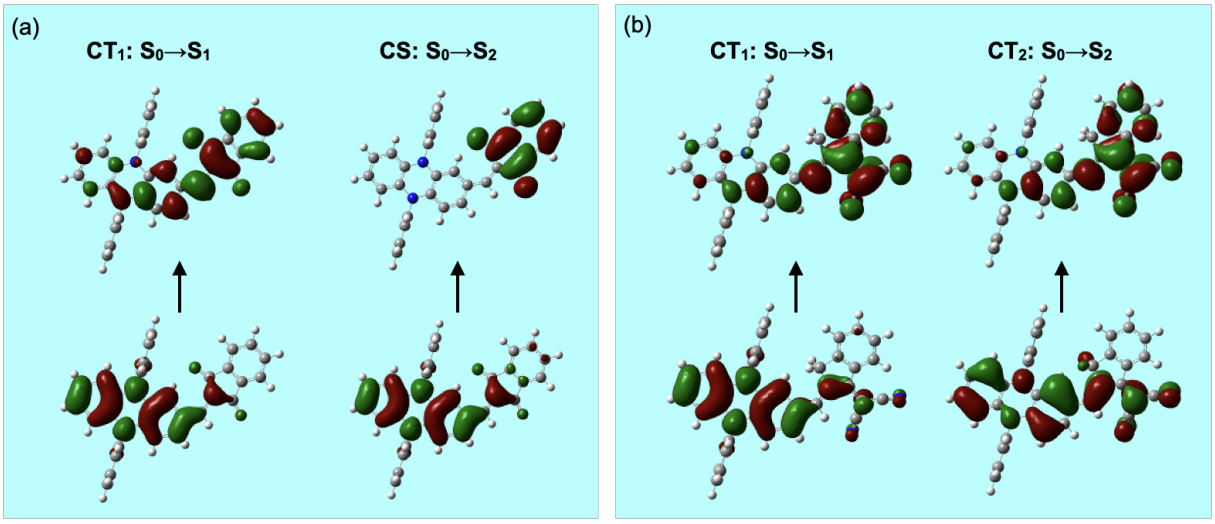

Figure S4*: Hole (down) and particle (up) natural transition orbitals pairs of (a)* ***DPPZ-IOO*** *and (b)* ***DPPZ-ID*** *for $S_0 \rightarrow S_1$ (HOMO→LUMO) and $S_0 \rightarrow S_2$ (****DPPZ-IOO****: HOMO→LUMO+1,* ***DPPZ-ID****: HOMO−1→LUMO) transitions, calculated with TD DFT at the B3LYP/6-31G(d,p) with PCM ($CHCl_3$), isovalue 0.02.*

Geometry optimization in the S_1 state

In the S_1 state, B3LYP computations always converged to the nonplanar geometry, relating to twisted intramolecular charge transfer (TICT). While local minimums of the planar intramolecular charge transfer ($PICT_c$) with *s-cis* conformations were found only for **DPPZ-IO** and **DPPZ-IOO,** and local minimums of $PICT_t$ with *s-trans* conformation were also found for all four derivatives, even though very flat minimums for **DPPZ-ID** and **DPPZ-IDO** (Figure S4).

Consequently, **DPPZ-IO** and **DPPZ-IOO** have the rotational barrier in the S_1 state, while these twists of **DPPZ-ID** and **DPPZ-IDO** are barrierless. Although TICT state has a fully charge-separated electronic structure with marginal overlap of HOMO and LUMO NTOs, electronic transition to the S_1 state remains CT_1 character (HOMO→LUMO) not CS character (HOMO→LUMO+1), as confirmed by the same LUMO NTO shape localised on benzene part of indandione (Figures S3 and S5). In this case of B3LYP, CS state for **DPPZ-IDD** is probably the global minimum in the S_1 state, nevertheless the S_1-state geometry optimizations failed because of the small energy difference of CS geometry between S_1 and S_0 states. On the other hand, CAM-B3LYP transition energies from the S_1 state minimums relating to fluorescence are considerably higher than those of the B3LYP by about 0.5 eV, so as in the case of Franck-Condon transitions relating to the absorption (Table 2). And, as observed for the Franck-Condon transitions, B3LYP transition energies for *s-trans* conformers except for **DPPZ-IDO** are quite close to the experimental fluorescence maxima (Table S9).

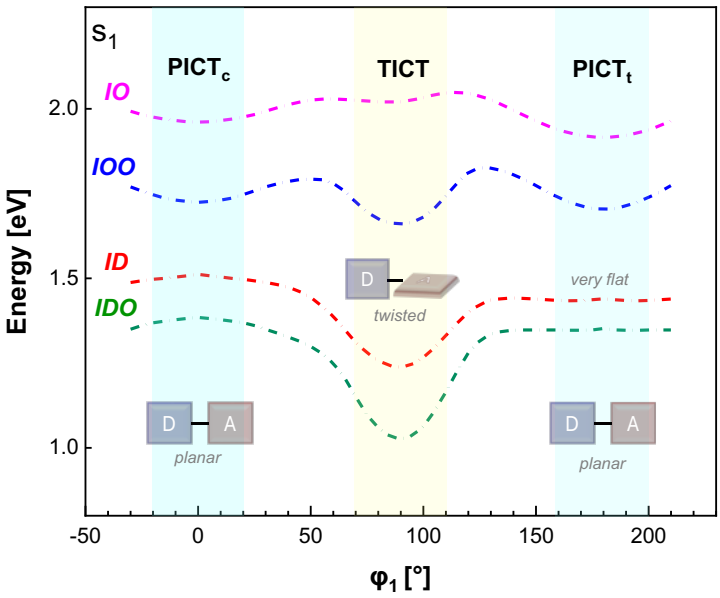

***Figure S5**. Energy dependence on the twist for **DPPZ-IO**, **DPPZ-IOO**, **DPPZ-ID** and **DPPZ-IDO** in the S_1 state calculated at the B3LYP/6-311G(d,p) with PCM ($CHCl_3$). Blue and yellow highlighted regions indicates $PICT_c$, $PICT_t$ and TICT minima.*

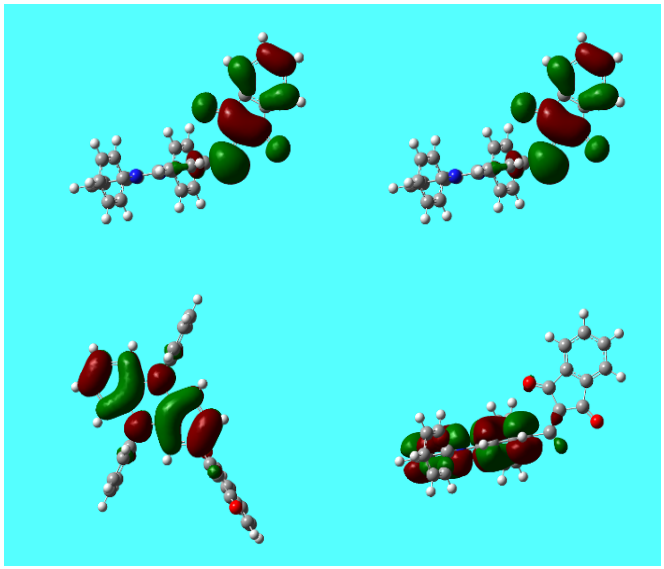

***Figure S6**: Hole (down) and particle (up) natural transition orbitals pair of **DPPZ-IOO** in TICT minimum relating to $S_1 \rightarrow S_0$ (HOMO→LUMO) transition, calculated with TD DFT at the B3LYP/6-311G(d,p) with isovalue of 0.02.*

***Table S9**: Summary of electronic transition energies (eV) of **DPPZ-EWD** with the minima geometry in the S_1 state calculated at the B3LYP/6-311G(d,p) with PCM ($CHCl_3$).*

Compound	$PICT_c$	TICT	$PICT_t$	Exp. [a]
DPPZ-IO	1.83	1.49	1.76	1.71
DPPZ-IOO	1.59	0.91	1.57	1.53
DPPZ-ID		0.71	1.29	1.36
DPPZ-IDO		0.35	1.08	~1.35

[a]Fluorescence maxima in $CHCl_3$ solution.

S7 UV-Vis-NIR absorption and fluorescence in solution and solid state

Table S10: *Optical properties in various environments.*

Compd.	Condition	Medium	Absorption		Fluorescence		Stokes shifts
			λ_{abs} [nm]	ε [$M^{-1}cm^{-1}$]	λ_{em} [nm]	Φ [%]	[cm^{-1}]
DPPZ-CHO	**Solution**	Cyclohexane	449, 480(sh)	5300	496, 530(sh)		672
		Toluene	458	5300	529, 551(sh)	60.0	2930
		1,4-dioxane	456	7600	540		3411
		THF	457	6000	540		3363
		$CHCl_3$	473	8900	588	3.0	4135
		CH_2Cl_2	469	8100	593		4459
		CH_3CN	463	10400	587		4562
	Doped film	PMMA	458		551	16.0	3685
	Neat film		469		580	4.7	4081
	Crystal	EtOAc/CH_2Cl_2			585	14.2	
DPPZ-IO	**Solution**	Cyclohexane	499, 529(sh)	12900	555, 598(sh)		885
		Toluene	517	15000	620	28.7	3213
		1,4-dioxane	516	13500	646		3899
		THF	520	13500	676		4438
		$CHCl_3$	541	12900	727		4729
		CH_2Cl_2	539	13100	750		5220
		CH_3CN	546	[a]	834		6325
	Doped film	PMMA	527		634	8.4	3202
	Neat film		545		725	[b]	4556
	Crystal	CH_2Cl_2/*n*-hex			717	4.0	
DPPZ-DCV	**Solution**	Cyclohexane	553, 593(sh)	3300 [a]	625		863
		Toluene	572	16200	672	9.0	2602
		1,4-dioxane	568	6200 [a]			
		THF	577	17000	711		3266
		$CHCl_3$	596	16700	717	2.2	2832
		CH_2Cl_2	593	14700	726		3089
		CH_3CN	582	19700	744		3741
	Doped film	PMMA	580		706	0.4	3077
	Neat film		613		761	1.0	3173
	Crystal	$CHCl_3$/*n*-hex			736	0.2	
		EtOAc/*n*-hex			785		
DPPZ-IOO	**Solution**	Cyclohexane	598(sh), 645	29300	676, 738(sh)		711
		Toluene	634	27400	734	3.0	2149
		1,4-dioxane	624	15140 [a]	770		3038
		THF	633	24000	793		3187
		$CHCl_3$	655	20100	812	0.3	2952
		CH_2Cl_2	651	21000	826		3254
		CH_3CN	639	26500	843		3787
	Doped film	PMMA	636		743	1.1	2264
	Neat film		665		843	0.2	3266
	Crystal	$CHCl_3$/MeOH			786	1.1	
DPPZ-ID	**Solution**	Cyclohexane	632(sh), 673	14200	717, 789(sh)		912
		Toluene	672	20400	821	[b]	2701
		1,4-dioxane	660	18300	862		3551
		THF	680	23300	945		4124
		$CHCl_3$	695	19400	915	[b]	3460
		CH_2Cl_2	692	17300	964		4077
		CH_3CN	687	[a]	[b]		
	Doped film	PMMA	670		[b]	[b]	
	Neat film		735		[b]	[b]	
	Crystal	$CHCl_3$			975		

[a] Low solubility. [b] Too low signal. Continue to the next page.

Table S10: (Continued from the former page)

Compd.	Condition	Medium	Absorption λ_{abs} [nm]	Absorption ε [$M^{-1}cm^{-1}$]	Fluorescence λ_{em} [nm]	Fluorescence Φ [%]	Stokes shifts [cm^{-1}]
DPPZ-IDO	**Solution**	Cyclohexane	695(sh), 759	12500 [a]	823	[b]	1025
		Toluene	748	27200	886		2082
		1,4-dioxane	735	25200	917		2700
		THF	748	28900	932		2639
		$CHCl_3$	778	25400	922	[b]	2007
		CH_2Cl_2	769	24300	955		2533
		CH_3CN	753	9600 [a]	[b]		
	Doped film	PMMA	748		834		1379
	Neat film		804		1012		2556
	Crystal	EtOAc/*n*-hex			1100	[b]	
DPPZ-IDD	**Solution**	Cyclohexane	838	10500	954		1451
		Toluene	847	13900	963	[b]	1422
		1,4-dioxane	833	11800			
		THF	831	17000	[b]		
		$CHCl_3$	880	21500	[b]		
		CH_2Cl_2	850	24500	[b]		
		CH_3CN	827	13600	[b]		
	Doped film	PMMA	795		[b]	[b]	
	Neat film		931		[b]	[b]	

[a] Low solubility [b] Too low signal

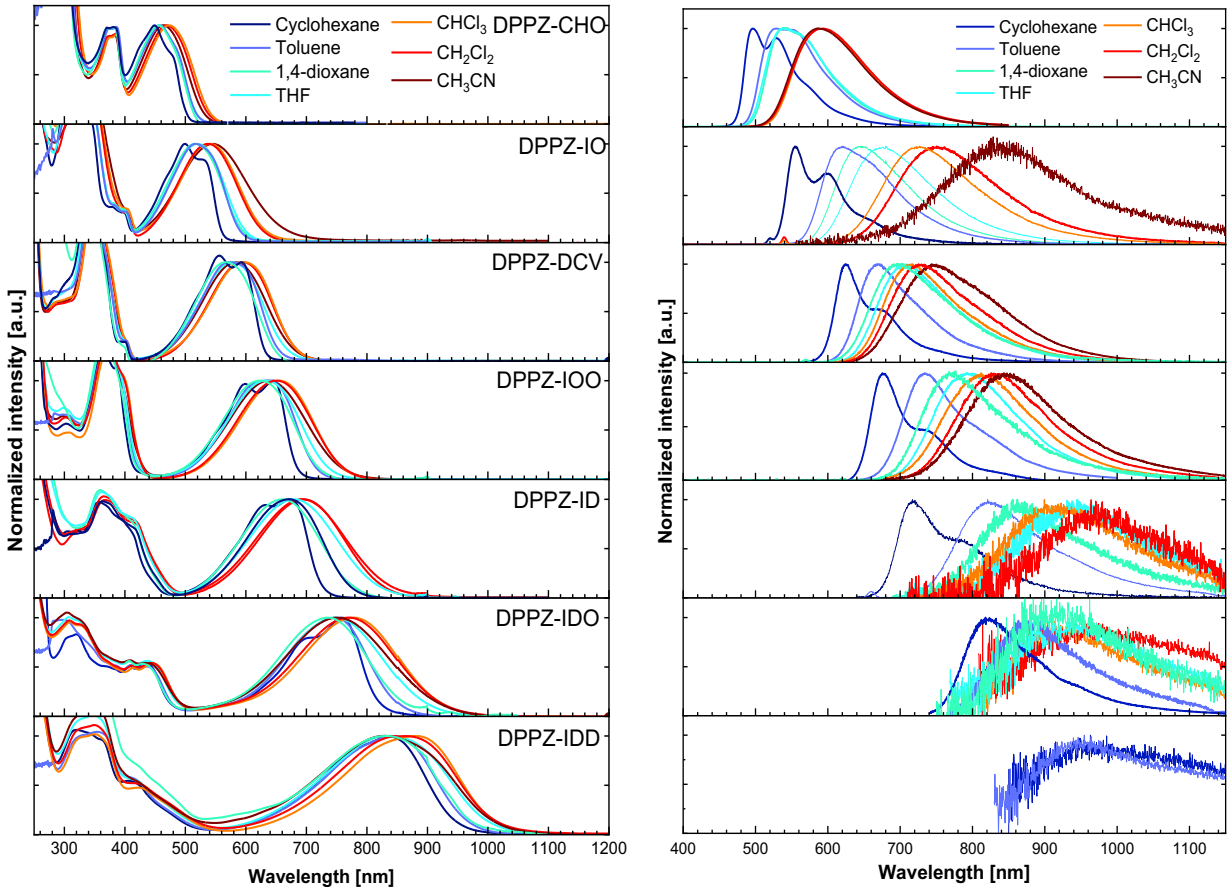

Figure S7: Normalized absorption (left) and fluorescence spectra (right) of **DPPZ-EWG** in various solvents (c = 3 × 10^{-5} mol/L).

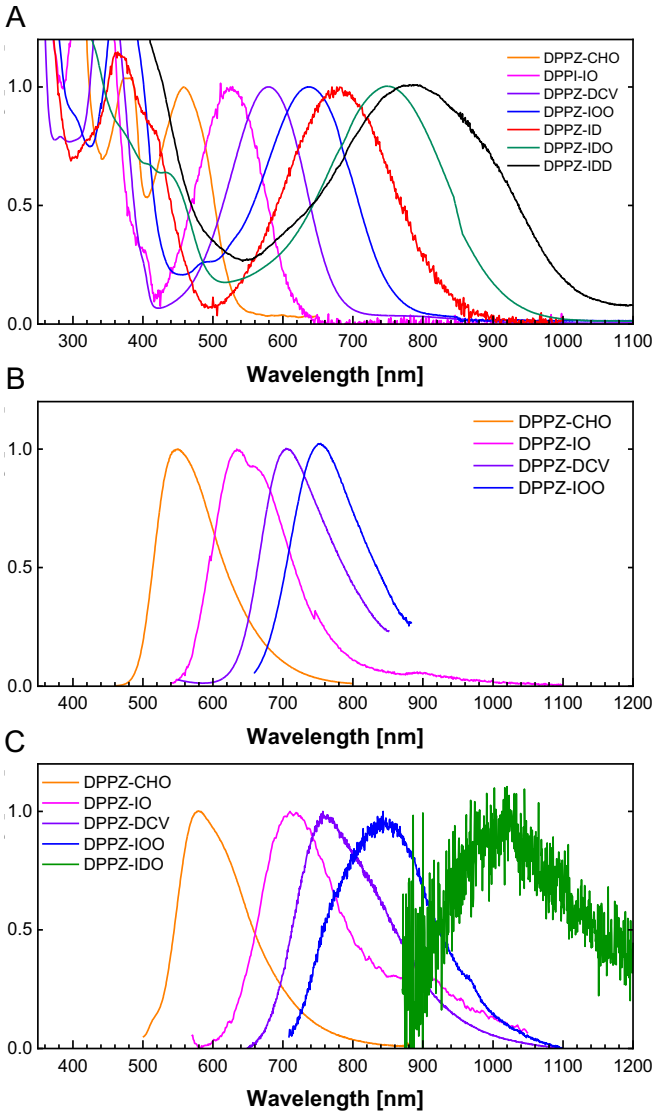

Figure S8: *(A) Absorption and fluorescence spectra of (B) PMMA films and (C) amorphous neat films.*

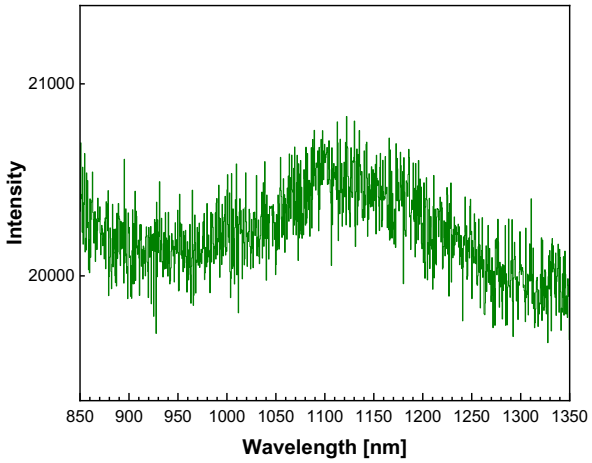

Figure S9: *Fluorescence spectrum of polycrystalline* ***DPPZ-IDO****.*

S8 pXRD

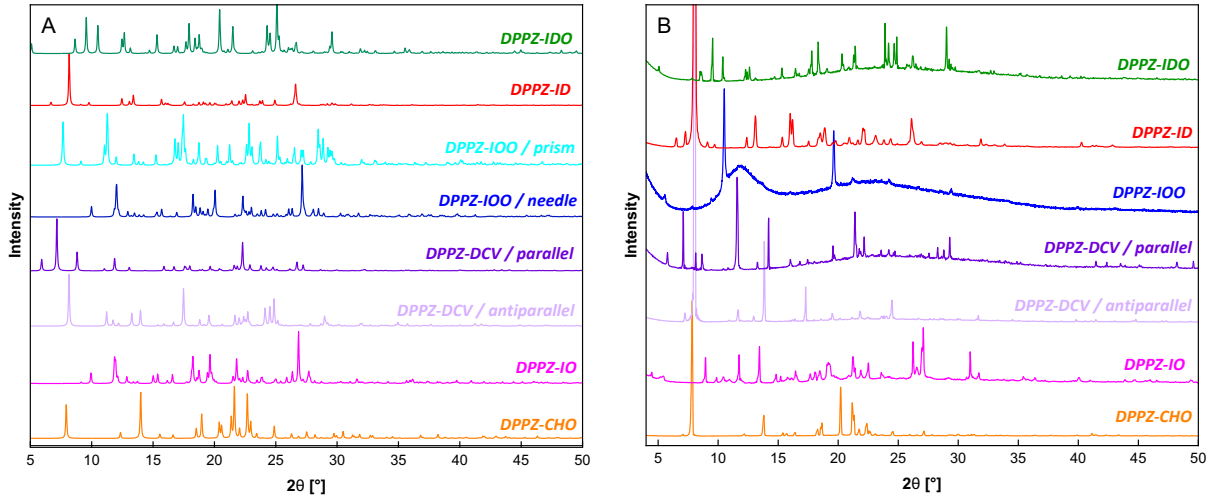

Figure S10: *(A) Simulated and (B) experimental pXRD patterns of polycrystalline powders.* ***DPPZ-IOO*** *sample was measured as a mixture of prismatic and needle crystals.*

S9 Stability

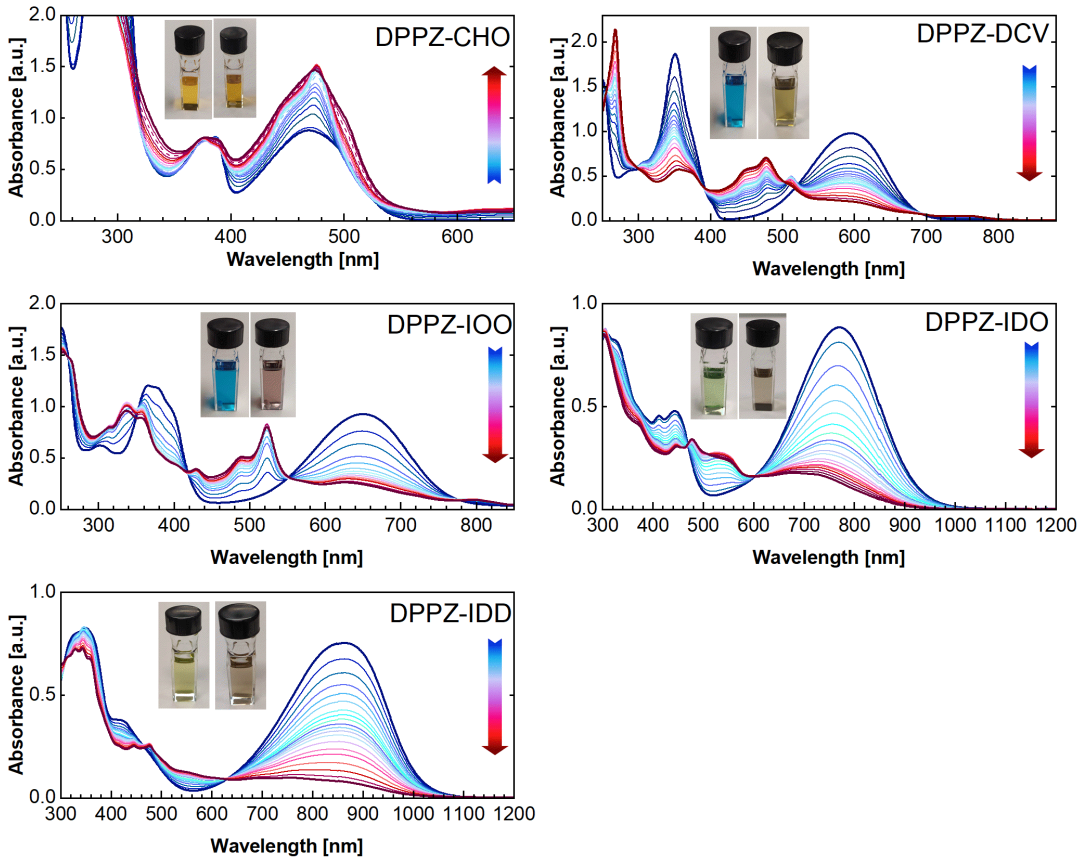

Figure S11*: Absorption spectral changes by UV irradiation time in CH_2Cl_2 solution.*

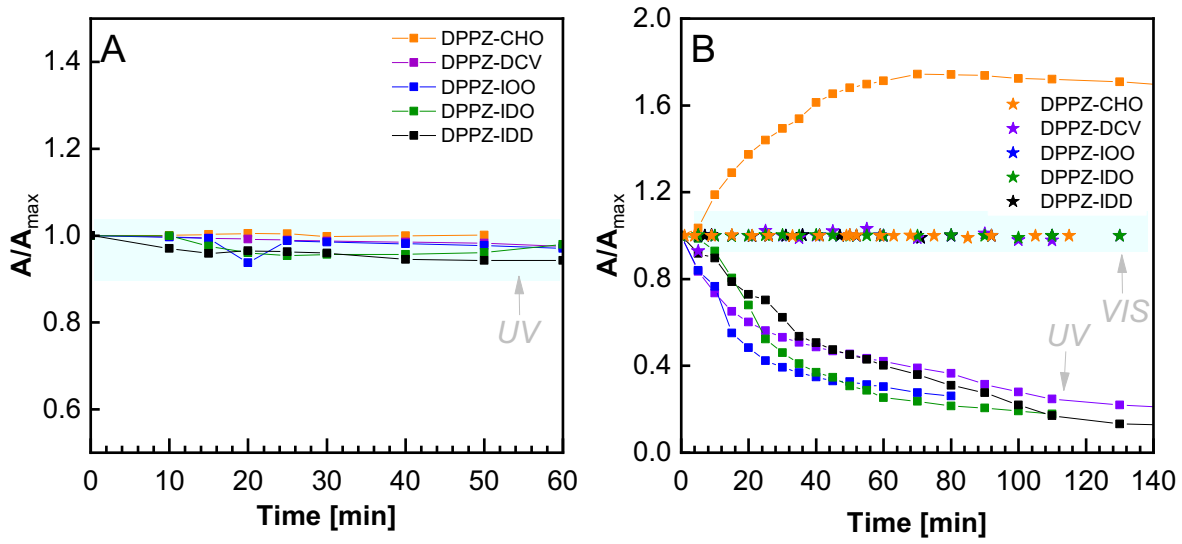

***Figure S12**: Change of A/A_{max} in time after UV and VIS light irradiation for (A) neat* film, *(B) CH_2Cl_2 solution.*

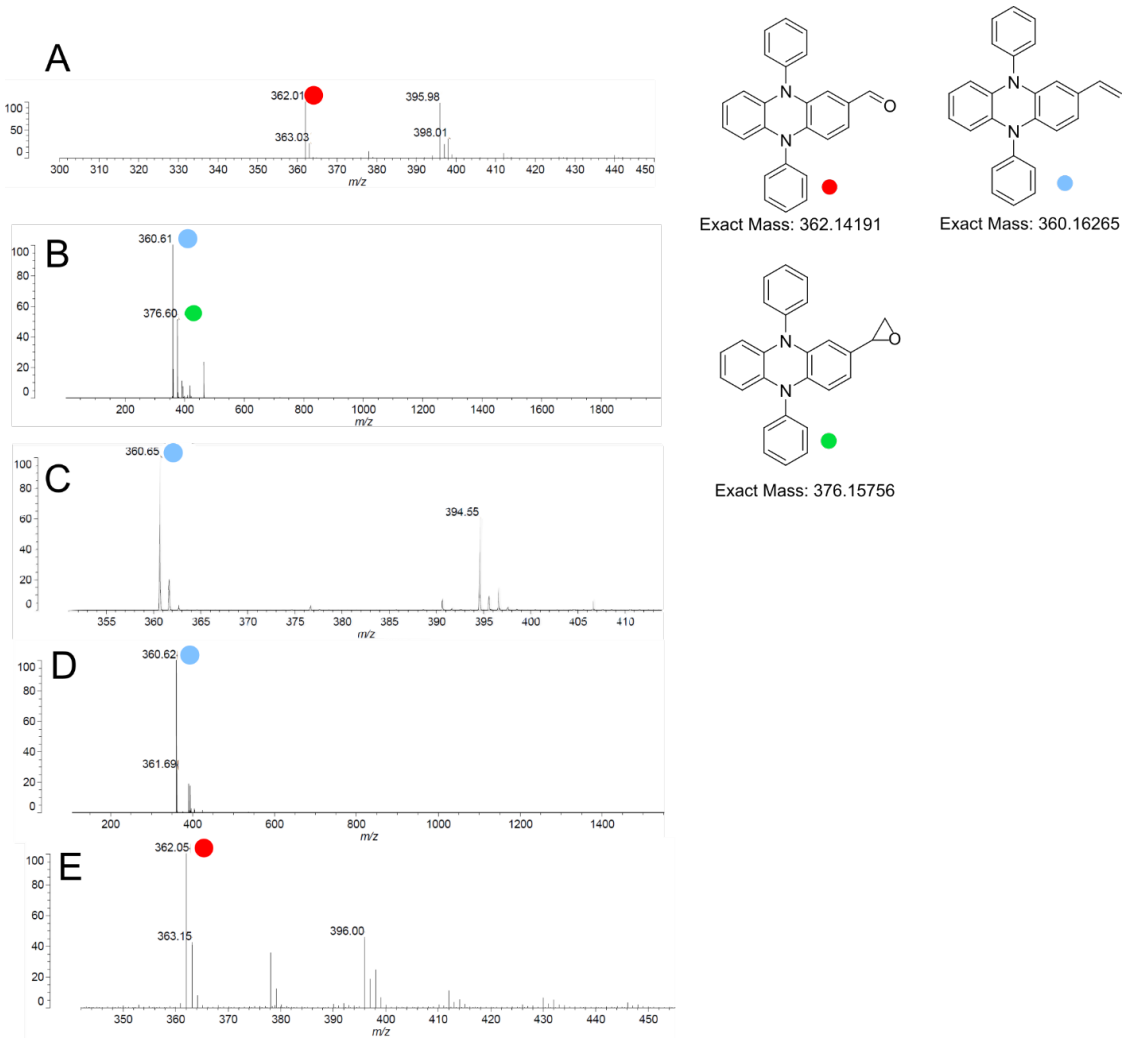

***Figure S13**: MS of recovered samples after UV irradiation for **DPPZ-CHO** (A), **DPPZ-DCV** (B), **DPPZ-IOO** (C), **DPPZ-IDO** (D), **DPPZ-IDD** (E).*

S10 References

[S1] D. Püschel, J. Wiefermann, S. Hédé, T. Heinen, L. Pfeifer, O. Weingart, M. Suta, J. J. T. Müller, C. Janiak. *J. Mater. Chem. C*, **2023**, *11*, 8982–8991.

[S2] T. Okamoto, E. Terada, M. Kozaki, M. Uchida, S. Kikukawa, K. Okada. *Org. Lett.* **2003**, *5*, 373–376.

[S3] X. Chen, Z. Zhao, Y. Liu, P. Lu, Y. Wang. *Chem. Lett.* **2008**, *37*, 570–571.

[S4] M. Planells, N. Robertson, *Eur. J. Org. Chem*. **2012**, 4947–4953.

[S5] L. Krause, R. Herbst-Irmer, G. M. Sheldrick, D. Stalke, *J. Appl. Cryst*. **2015**, 48, 3–10.

[S6] S. Luňák Jr., T. Aysha, A. Lyčka, O. Machalický, R. Hrdina, *Chem. Phys. Lett*. **2014**, *608*, 213–218.

[S7] a) D. K. A. Phan Huu, R. Dhali, C. Pieroni, F. Di Maiolo, C. Sissa, F. Terenziani, A. Painelli, *Phys. Rev. Lett*. **2020**, *124*, 107401; b) D. K. A. Phan Huu, C. Sissa, F. Terenziani, A. Painelli, *Phys. Chem. Chem. Phys*. **2020**, *22*, 25483–25491.

[S8] C. Adamo, D. Jacquemin, *Chem. Soc. Rev*. **2013**, *42*, 845–856.

[S9] A. A. Isse, A. Gennaro, *J. Phys. Chem. B* **2010**, *114*, 7894–7899.